Microfabrication Strategies for the Patterning of Biodegradable Substrate

by

Elif Yaren Özüaçıksöz

A Dissertation Submitted to the
Graduate School of Sciences and Engineering
in Partial Fulfillment of the Requirements for
the Degree of

Master of Science

in

Biomedical Sciences and Engineering

KOÇ
ÜNİVERSİTESİ

October 18, 2023

Microfabrication Strategies for the Patterning of Biodegradable Substrate

Koç University

Graduate School of Sciences and Engineering

This is to certify that I have examined this copy of a master's thesis by

Elif Yaren Özüaçıksöz

and have found that it is complete and satisfactory in all respects,
and that any and all revisions required by the final
examining committee have been made.

Committee Members:

_____

Asst. Prof. Serap Aksu Ramazanoğlu (Advisor)

_____

Assoc. Prof. Ekin Aslan

_____

Assoc. Prof. Caner Ünlü

Date: October 18, 2023

To my family…

ABSTRACT

Microfabrication Strategies for the Patterning of Biodegradable Substrate

Elif Yaren Özüaçıksöz

Master of Science in Biomedical Sciences and Engineering

October 18, 2023

Replacing the non-degradable materials with the biodegradable ones is a crucial strategy for removing environmental waste and boosting eco-friendly practices. In this sense, in the recent years, both in the medicine and industry, non-degradable materials are being replaced with their degradable alternatives. Cell culturing applications, drug delivery applications, and fabrication of other implantable medical devices are some examples where the biodegradable alternative materials are highly desired.

The processability of the biodegradable substrates significantly depend on the microfabrication method that is chosen to process it. For this reason, in order to make use of the biodegradable materials, providing a detailed examination of the microfabrication strategies for the patterning of biodegradable substrates is very critical.

This thesis investigates the conventional and unconventional fabrication methods to craft microstructures on biodegradable PLA substrate. As the PLA is a very sensitive biodegradable material, the use of conventional microfabrication methods such as photolithography, microstamping, and laser ablation is very limited in the laboratory as well as in the industry. In this work, stencil lithography using DRIE-based Si-stencils for both PLA etching and material deposition simultaneously are utilized. In addition to separately etching and depositing metals on substrates, a molybdenum electrode embedded inside PLA substrate is demonstrated. While the average resistance is measured as 796.45 Ω when the electrodes are on top of PLA substrate, the average resistance is measured as 2.0297 kΩ when the electrodes are embedded inside the PLA substrate due to the roughness caused by etching. Overall, we provide a handbook to wisely select a protocol for large area and high throughput fabrication of any microstructure on PLA biodegradable substrate, which can be extended to a variety of other sensitive biodegradable materials.

ÖZETÇE

Biyobozunur Substrat Modellenmesi için Mikrofabrikasyon Stratejileri

Elif Yaren Özüaçıksöz

Biyomedikal Bilimler ve Mühendisliği, Yüksek Lisans

18 Ekim 2023

Biyobozunur olmayan malzemelerin biyobozunur malzemelerle değiştirilmesi, çevresel atıkların ortadan kaldırılması ve çevre dostu uygulamaların desteklenmesi açısından çok önemli bir stratejidir. Bu anlamda son yıllarda hem tıpta hem de endüstride biyobozunur olmayan malzemelerin yerini biyobozunur alternatifleri alıyor. Hücre kültürü uygulamaları, ilaç salınımı uygulamaları ve vücutta kullanılacak diğer tıbbi cihazların imalatı, biyobozunur alternatif malzemelerin oldukça arzu edildiği bazı örneklerdir.

Biyobozunur substratların işlenebilirliği, onu işlemek için seçilen mikro üretim yöntemine önemli ölçüde bağlıdır. Bu nedenle biyobozunur malzemelerden faydalanmak için biyolojik olarak parçalanabilen substratların desenlendirilmesine yönelik mikrofabrikasyon stratejilerinin ayrıntılı bir şekilde incelenmesi çok önemlidir.

Bu tez, biyolojik olarak parçalanabilen PLA substratı üzerinde mikro yapılar oluşturmak için geleneksel ve alışılmadık üretim yöntemlerini ele almaktadır. PLA çok hassas bir malzeme olduğundan, fotolitografi, mikro damgalama ve lazer ablasyon gibi geleneksel mikro imalat yöntemlerinin laboratuvarda veya endüstride kullanımı çok sınırlıdır. Bu çalışmada, hem PLA aşındırma hem de malzeme biriktirme için aynı anda DRIE bazlı Si şablonları kullanan şablon litografisinden yararlanıldı. Metallerin alt katmanlar üzerine ayrı ayrı aşındırılması ve biriktirilmesine ek olarak, PLA alt katmanının içine gömülü bir molibden elektrodu da gösterildi. Elektrotlar PLA substratının üzerindeyken ortalama direnç 796,45 Ω olarak ölçülürken, aşındırma işleminin neden olduğu pürüzlülük nedeniyle elektrotlar PLA substratı içerisine gömüldüğünde ortalama direnç 2,0297 kΩ olarak ölçüldü. Bu tez ile genel olarak, biyolojik olarak bozunabilir PLA substrat üzerindeki herhangi bir mikro yapının geniş alanlı ve yüksek verimli üretimi için bir protokolün akıllıca seçilmesine yönelik bir el kitabı sağlıyor ve diğer çeşitli hassas biyolojik olarak bozunabilir malzemelere de genişletilebilecek yöntemler sunuyoruz.

ACKNOWLEDGEMENTS

I want to start by thanking my advisor, Serap Aksu Ramazanoğlu, in the most sincere way possible for all the support throughout my master's period. Not only she has supported me during this period both academically and personally, but also she showed me how an academician can both be very good hearted, talented, and successful. Although graduate study period is known as an extremely tough period both academically and personally, she made it as easy as it can be for me by giving all type of support that she can provide by all her means, and she always continues to provide it to all her students. I feel very lucky that I got the chance to meet with her and became her student for my master's studies.

I would like to express my sincere appreciation to my lifelong colleague and partner, dearest Mohammadjavad Bathaei, for all the support he provided me, all the understanding he showed to me during tough times, and for always making me smile. I would like to thank him for sharing all his experience which helped me to make my way to this day and thank him for walking this way beside me.

Moreover, I would like to thank all my friends who supported me and made my life much better throughout this journey. More importantly, I should thank my mom and dad for never withdrawing their support from my life. I would not be able to make it until this day without their precious help and support in every step of my life.

Finally, I would like to thank Koç University Surface Science and Technology Center **(**KUYTAM) and Nanofabrication and Nanocharacterization Center for Scientific and Technological Advanced Research (n^2STAR) teams for their support for my master studies and providing all the facilities which made this thesis possible. And I also would like to thank The Scientific and Technological Council of Turkey (TÜBİTAK) for the financial support.

TABLE OF CONTENTS

LIST OF TABLES

LIST OF FIGURES

ABBREVIATIONS

IMDs	Implantable Medical Devices
UV	Ultraviolet
DRIE	Deep Reactive-Ion Etching
PLA	Polylactic Acid
PGS	Poly(glycerol sebacate)
PDMS	Polydimethylsiloxane
AFM	Atomic Force Microscopy
SWNTs	Single-Walled Carbon Nanotubes
DOD	Drop-On-Demand
PEDOT:PSS	Poly(3,4-ethylenedioxythiophene) Polystyrene sulfonate
POC	Point-Of-Care
PVD	Physical Vapor Deposition
PI	Polyimide
RIE	Reactive Ion Etching
ICP-RIE	Inductively Coupled Plasma-Reactive Ion Etching
RF	Radiofrequency
HMDS	Hexamethyldisilazane
PBS	Phosphate-Buffered Saline

Chapter 1:
INTRODUCTION

Microfabrication strategies that are utilized for the patterning of flexible and stretchable biodegradable substrates represent a novel class of technology that allow the fabrication of biodegradable implantable medical devices (IMDs) and environmentally friendly, recyclable membranes [1]–[4]. Microfabrication strategies that are used to develop biodegradable IMDs and membranes greatly benefit from their unique features such as having small physical footprint and being eco-friendly, conformally adhering to the host tissue while maintaining their working capabilities (e.g., electrical properties) under mechanical loading, and dissolving within bodily fluids [5]–[8].

IMDs are only utilized in life-or-death situations in modern medicine due to the need for a subsequent retrieval surgery that entails additional risks for the patient, as well as financial costs for the clinician and the government. Without the need for additional IMD extraction procedures, biodegradable IMDs are expected to provide incredible novel possibilities for diagnostic, telemetry, and therapeutic IMDs [9]–[12]. A biodegradable and implantable cardiac pacemaker can be seen in Fig. 1.1.

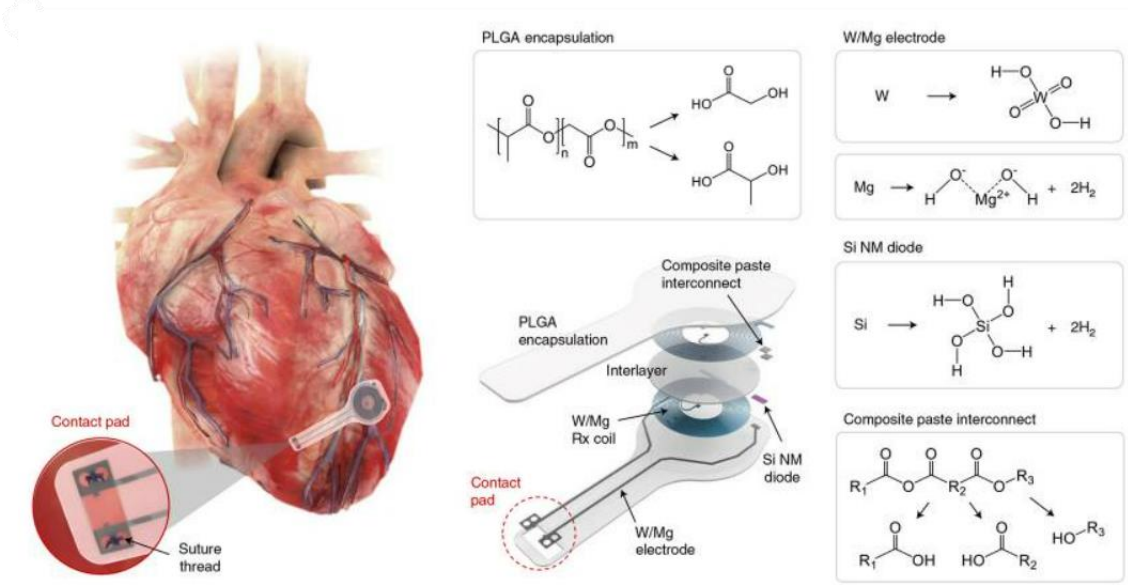

Figure 1.1: Illustration of a fully biodegradable and battery-free cardiac pacemaker, together with the degradation mechanisms of the materials used. Taken with permission from [5].

In addition to this, environmental waste problems caused by single-use biomedical devices and single-use gadgets are becoming more and more prevalent. Thus, eco-friendly alternatives such as biodegradable gadgets that quickly break down into recyclable byproducts have the potential to become a key in eliminating environmental concerns [13]–[15]. A biodegradable brain probe fabricated for the detection of neurotransmitters can be seen as an example in Fig. 1.2.

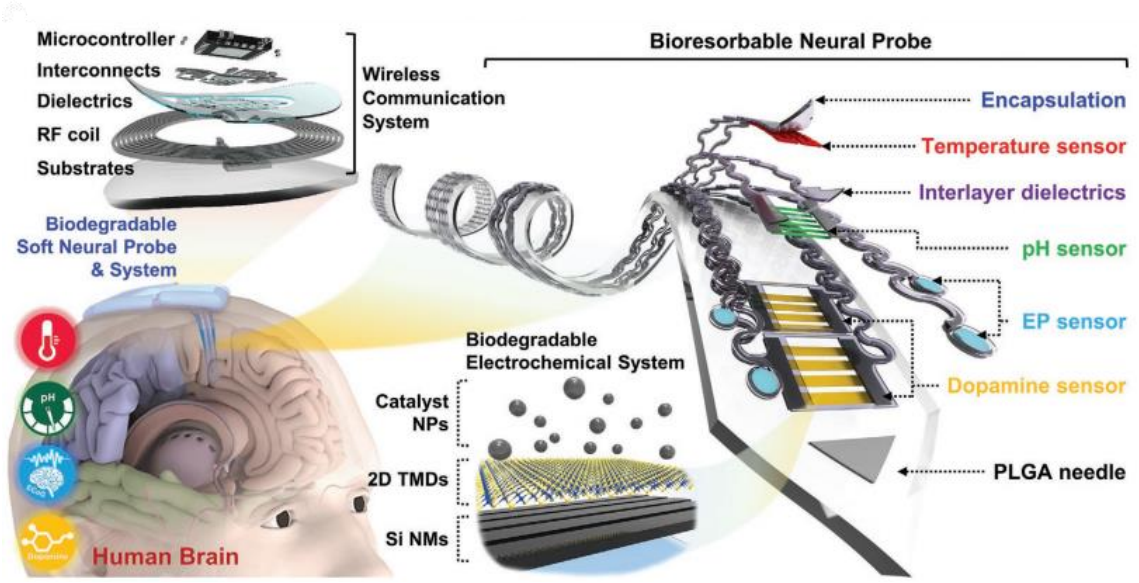

Figure 1.2: Illustration of a fully biodegradable Si-based brain probe for the detection of neurotransmitters, composed of Si NMs as electrode, Fe NPs as catalyst, MoS_2 and WS_2 for charge transfer, and PLGA microneedles for insertion. Taken with permission from [16].

Patterning of biodegradable materials finds various applications in medicine as well as in industry. In tissue engineering applications, it is vital to ensure that the cells are cultured in the proper place that they can grow, differentiate, and generate new tissues. The devices that the cells are implanted with are known as scaffolds and in order to have an efficiently working device, the scaffolds should be designed by considering the cell attachment, mechanical stability, and biocompatibility. Microfabrication strategies for the patterning of biodegradable materials are utilized for designing the scaffolds for a better cell adhesion and localized substance immobilization [17]. An example of a

micropatterned structure using femtosecond laser for scaffold preparation can be seen in Fig. 1.3.

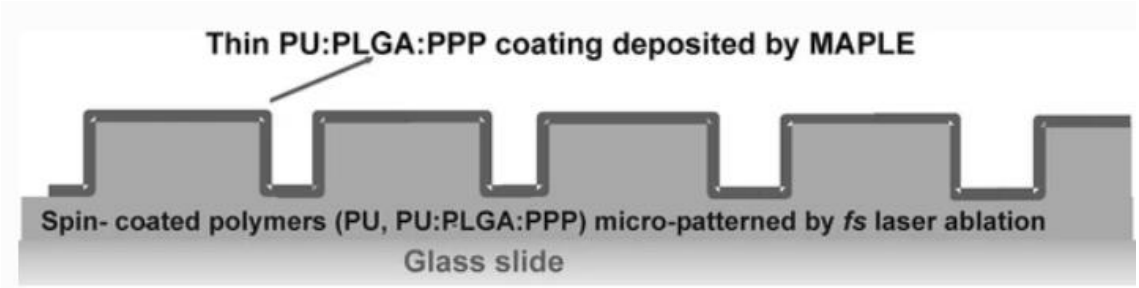

Figure 1.3: Micropatterned structures using laser ablation method for the scaffold preparation. Taken with permission from [17].

Fabrication of microholes for biomedical filters is challenging by using conventional fabrication methods. Thus, the same microfabrication strategies are also used for the fabrication of biomedical filters for cell culturing microfluidic devices for the improvement of permeability to the cell culture space [18].

In addition to the cell culturing features, controllably patterning biodegradable materials can be used in drug delivery applications. In this sense, the drug release is controlled by the size and the number of the pores of the material that the drug is encapsulated with [19]. An example of a biodegradable PLGA based microneedle used for drug delivery applications can be seen in Fig. 1.4.

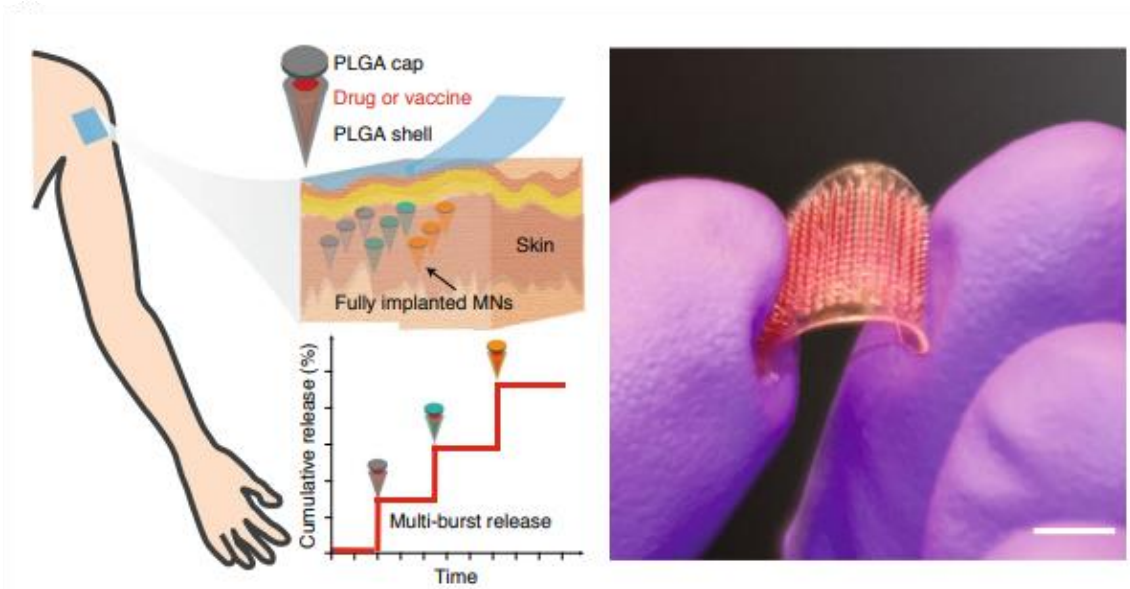

Figure 1.4: A PLGA based microneedle used for drug delivery applications. Taken with permission from [20].

Another application where the micropatterning of biodegradable materials becomes important is the filtering applications for material separation. Filters having certain size microholes that are fabricated using microfabrication methods are commonly used for the wastewater purification [21]. Changing these non-degradable filters to biodegradable alternatives would be a crucial strategy for eliminating the environmental waste and supporting greener approaches.

In order to successfully develop micropatterned biodegradable substrates to address certain applications, it is very important to choose the microfabrication strategy that will be used for the patterning of the biodegradable substrate. Most of the conventional microfabrication techniques are silicon (Si)-based and the biodegradable polymers that can be used as substrates are extremely vulnerable to organic solvents, plasma environments, thermal loading, and ultraviolet (UV) light [22]. Thus, it is important to investigate the standard microfabrication strategies and implement them into the traditional patterning, etching, and deposition methods for the creation of biodegradable flexible and stretchable gadgets.

This thesis aims to investigate the possible microfabrication strategies that can be used for the patterning of biodegradable polymers. Hence, firstly, biodegradable polymers that can be used for device microfabrication and their properties will be explained. Secondly, potential microfabrication strategies such as photolithography, stamping, laser engraving, and stencil lithography, will be demonstrated for the patterning of biodegradable substrates by sharing the benefits and the drawbacks of each of the methods. After that, the usage of deep reactive-ion etching (DRIE)-based Si-stencil for the patterning of biodegradable substrates will be investigated more in detail along with other applications of the fabricated DRIE-based Si-stencils. The focus of this thesis will be demonstrating the advantages and disadvantages of several microfabrication strategies for the patterning of biodegradable substrates and showing different applications of the DRIE-based Si-stencils as hard masks.

Advancements in biodegradable materials which can be resorbed by biological fluids and dissipate after a certain period of time enables the fabrication of biodegradable IMDs that allow the detection and treatment of the diseases in their early stages [9]. On the other hand, other than biodegradable IMDs, biodegradable gadgets such as biodegradable filters for material separation are good alternatives in order not to damage the environment while working for a certain amount of time. Thus, a detailed investigation

must be done into the biodegradable materials that can be used for the microfabrication of devices for different applications.

Since all the devices need supporting material for constructing functional components on it, a substrate is the initial component to take into account and the material choice for the device creator is frequently based on mechanical compliance. Consequently, the substrate selection is mainly determined by the application requirements. Common biodegradable substrate materials can be seen in Table 1.1, along with the material types, properties, and degradation mechanisms and rate.

Table 1.1: Common biodegradable substrate materials. Taken with permission from [9].

Materials	Type	T_g [°C]	Degradation mechanism and rate	Young's modulus [GPa]
Porous Si	Inorganic	–	Hydrolysis: (highly dependent on pore size and density)	Depending on porosity (0.87–50.9)
Cellulose	Natural polymer	250	Enzymatic: ≈0.3 nm min^{-1}	135
Chitosan	Natural polymer	140–150	Enzymatic: 0.7 mm thickness (80% weight loss in 20 days)	65
Peptides	Natural polymer	–	Enzymatic: 100 nm thickness (90% weight loss in 20 h)	20
Chitin	Natural polymer	236	Enzymatic: 150 µm thickness (60% weight loss in 25 h)	41
Silk	Natural polymer	200–240	Enzymatic: (40% weight loss in 25 days)	23
Dextran-based hydrogel (≈50%)	Natural polymer	172.5	Hydrolysis: (90% weight loss in 9 days)	≈0.000015
PLGA	Synthetic polymer	37	Hydrolysis: (≈100% weight loss in 50 days)	0.092
PVA	Synthetic polymer	77	Hydrolysis: –	0.00032
PGA	Synthetic polymer	34–40	Hydrolysis: 0.1 mm thickness (≈40% weight loss in 20 days)	7
PHBV	Synthetic polymer	5	Hydrolysis: (≈2.5% weight loss in 250 days)	0.2315
DTE carbonate	Synthetic polymer	90	Hydrolysis: (≈70% weight loss in 20 weeks)	1.471
PEO	Synthetic polymer	−56	Hydrolysis: (≈90% weight loss in 8 weeks)	0.65
POC	Synthetic polymer	–	Hydrolysis: (≈100% weight loss in 35 days)	0.00014
PPS	Synthetic polymer	≈80	Hydrolysis: (≈8% weight loss in 10 days)	3.7

Due to its degrading mechanism being similar to that of bulk Si, mainly dissolution through hydrolysis and the production of orthosilicic acid ($Si(OH)_4$)as the final product, porous silicon (pSi) which is an inorganic material, as a substrate, has attracted significant attention [23], [24]. Pore size and density have a significant impact on the degradation rate of pSi [25]. Although porous Si is biocompatible and biodegradable, its brittle nature severely restricts its suitability for nonconformal devices. Consequently, these substrates are utilized when a rigid backing substrate is required [24].

Although pSi has the advantages of providing impermeability and dimensional stability, they have the disadvantages of providing tunable material properties. In this situation, polymers having adjustable dissolution rates and mechanical features become

more appealing. Due to their highly adjustable dissolution rates [26], excellent biocompatibility [27], and environmentally friendly manufacturing processes [28], natural polymers are gaining lots of attention. When a natural polymer is regarded as a substrate, thermal and mechanical stability together with solvent compatibility are significant parameters to be considered. Additionally, several naturally derived materials, such as plant-based polysaccharides and animal-derived polymers have been utilized as substrates because of their inherent enzymatic degradability [9].

Another category of biodegradable materials, synthetic polymers, can be regarded as a good option considering the flexibility and stretchability features of the synthetic polymers depending on the application. Moreover, these polymers are usually fabricated through straightforward methods using relatively inexpensive fabrication strategies [9]. Substrates composed of flexible poly(l-lactic) acid (PLLA) and poly(caprolactone) (PCL), flexible and stretchable poly(glycerol sebacate) (PGS), poly(1,8-octanediol-co-citrate) (POC), poly(lactic-co-glycolic acid) (PLGA) are some examples for the synthetic biodegradable polymers existing in the literature.

In most of the sensory devices, electrical components like resistors, capacitors, and inductors are composed of conductive materials, which serve as the functioning parts of sensors and actuators. In addition to the substrate material choice, choosing a proper biodegradable conductive material is a vital step for the fabrication of biodegradable sensors, which should be done considering the application and the fabrication method. Common biodegradable conductive materials can be seen in Table 1.2, along with the material types, degradation mechanisms and rate, and suitable fabrication method.

Table 1.2: Common biodegradable conductive materials. Taken with permission from [9].

Materials	Type	Degradation mechanism and rate	Fabrication method
Highly doped Si-nanomembrane	Inorganic	Hydrolysis: ≈11 nm day^{-1}	SOI wafer + solid state diffusion
Mg	Inorganic	Hydrolysis: $Mg + 2H_2O \rightarrow Mg(OH)_2$ 1700 nm day^{-1}	Thermal evaporation
Mo	Inorganic	Hydrolysis: $2Mo + 2H_2O + 3O_2 \rightarrow 2H_2MoO_4$ 20 nm day^{-1}	Sputtering deposition
Zn	Inorganic	Hydrolysis: $Zn + 2H_2O \rightarrow Zn(OH)_2 + H_2$ 3500 nm day^{-1}	Magnetron sputtering deposition
W	Inorganic	Hydrolysis: $2W + 2H_2O + 3O_2 \rightarrow 2H_2WO_4$ 150 nm day^{-1}	Electron beam deposition
Fe	Inorganic	Hydrolysis: $4Fe+3O_2 +10H_2O \rightarrow 4Fe(OH)_4 +4H$ ≈100 nm day^{-1}	Vacuum magnetron sputtering
PDPP-PD	Synthetic polymer	Hydrolysis: (100% weight loss in 11.5 h)	Polymerization
Dopant-free conductive polyurethane elastomer	Synthetic polymer	Hydrolysis and enzymatic: (12–14% weight loss in 8 weeks)	Polymerization
PGAP	Synthetic polymer	Hydrolysis: (≈50% weight loss in 70 days)	Polymerization
PPy/PLA	Composite	Hydrolysis: (≈25% weight loss in 12 weeks)	Electrospinning

Si is an inorganic biodegradable material which can be conductive through doping process. Depending on the doping temperature and level, the electrical conductivity of doped-Si can reach to 10^{-1}–10^{2} S cm^{-1} [29]. Other inorganic biodegradable materials, such as magnesium (Mg), molybdenum (Mo), zinc (Zn), tungsten (W), and iron (Fe) are also electrically conductive metal candidates that can be considered for biodegradable device fabrication. Among them, Mo, Zn, W, and Fe can be deposited using mostly standard deposition methods like sputtering and electron beam deposition. In addition to these metals, Mg has the advantages of being more electrically conductive and being easier to deposit [30]. The electrical conductivity of the aforementioned biodegradable materials can reach to 10^{7} S cm^{-1}, which makes them very desirable to use for the fabrication of biodegradable electrical components [29].

Another category of biodegradable conductive materials can be biodegradable polymers and their composites. They can be used in the form of biodegradable conductive paste for screen-printing or 3D-printing. Synthetic polymers, such as poly(diketopyrrolopyrrole-pphenylenediamine) (PDPP-PD) [31], dopant-free conductive polyurethane elastomer [32], poly[(glycine ethyl ester) (aniline pentamer) phosphazene] (PGAP) [33], and polypyrrole/ polylactic acid composite (PPy/PLA) [34] are some examples that can be found in the existing literature. Substrate materials, electrode materials, semiconductor materials, dielectric materials, encapsulation and adhesion

materials that can be chosen for the fabrication of biodegradable health monitoring devices can be seen as a summary in the schematic below (Figure 1.5) [35].

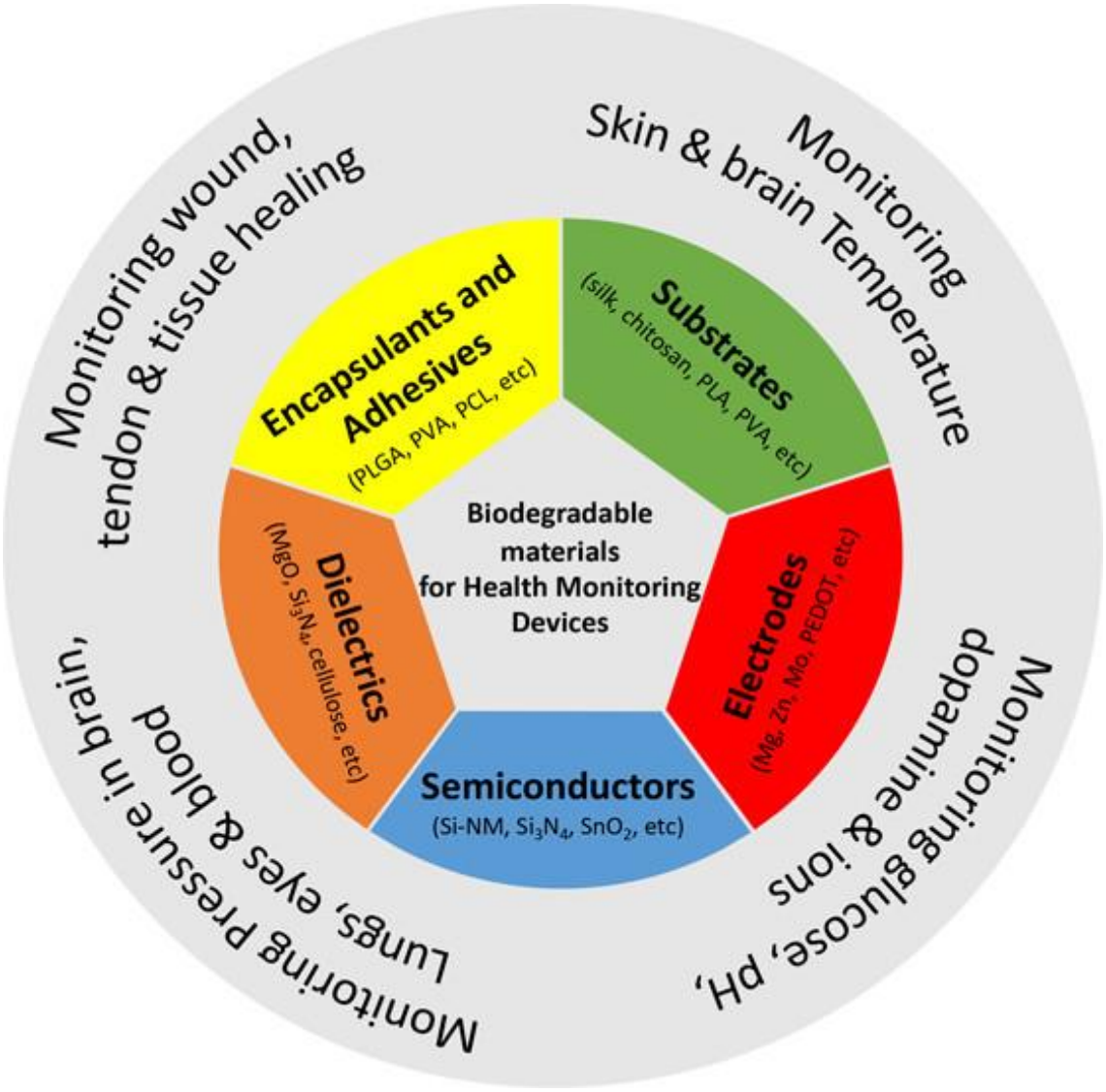

Figure 1.5: Common biodegradable materials for health monitoring devices. Taken with permission from [33].

Chapter 2:
CONVENTIONAL MICROFABRICATION STRATEGIES

In order to adapt biodegradable materials to conventional microfabrication methods for developing biodegradable devices and membranes, special microfabrication methods are required. In the case of IMDs, to be able maintain the desired operation of the implant with minimal damage to the biological system, the implants must match with the surrounding soft and curved tissues, which can only be possible by using soft and flexible materials as device substrates. On the other hand, since soft and flexible materials are not self-supporting, it can be tricky to develop devices using them [9]. The materials that are most commonly used for these applications are natural or synthetic biodegradable polymers, but typically, they lack sufficient resilience to high temperatures (such as during baking) and solvents used in conventional microfabrication stages (such as etchants, developers) [36]. Novel manufacturing procedures that are not only compatible with biodegradable materials but also suitable for low-cost mass production of biodegradable devices are being used to address these obstacles. The microfabrication methods most frequently used for device fabrication in the literature are photolithography, microstamping, laser ablation, stencil lithography, transfer printing, and inkjet printing. In order to fabricate biodegradable devices, aforementioned microfabrication methods should be updated and adapted in a way that it provides possibility to use biodegradable materials for biodegradable device development. In addition to this, transfer printing and inkjet printing methods can only be used for patterning on the substrate (such as patterning metal on the substrate) while microstamping method can only be used for patterning of the substrate (such as etching). Methods like photolithography, laser ablation, and stencil lithography can be used for both cases.

2.1 Photolithography

Photolithography is an optical technique which is used to transfer a pattern on a substrate, or to pattern a substrate directly. The first step in photolithography is to coat the substrate with photoresist. Secondly, the substrate is exposed to electromagnetic

radiation for placing the mask of the pattern which changes its molecular structure and results with the change in the solubility of the material. The third step is development of the photoresist, where the exposed resist is washed away while unexposed resist remains. The fourth step differs depending on the application of the device developer. Most commonly, it can either be deposition (usually a metal, semiconductor, or insulator) using evaporation or sputter tools followed by a lift-off process where the photoresist is removed and the desired features are remained on the substrate; or it can be etching (wet or dry) using chemicals or etching tools where the resist acts as a mask, and followed by the removal of the photoresist which leaves the desired features on the substrate. A typical photolithography process where Si wafer is used as a substrate can be seen in Fig. 2.1.

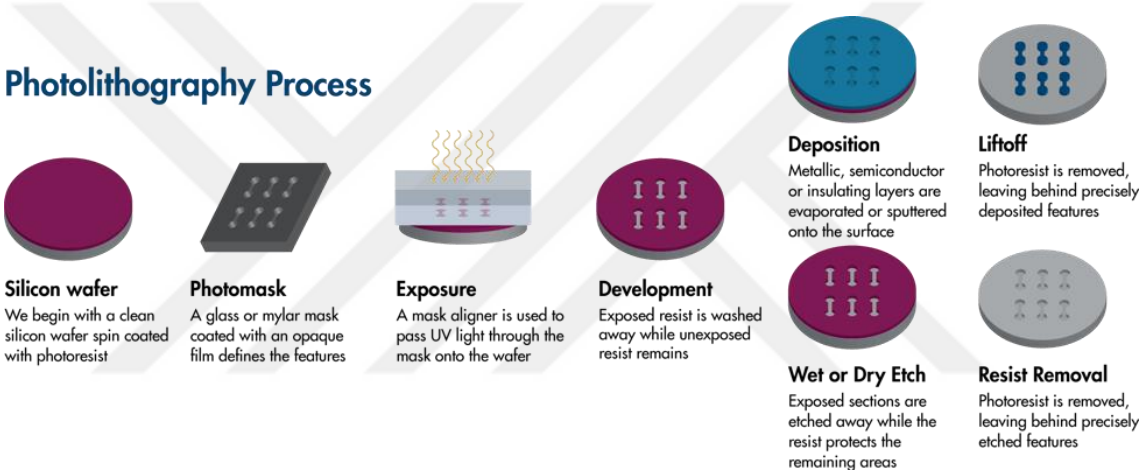

Figure 2.1: A conventional photolithography fabrication flow, using Si wafer as substrate. Taken with permission from [58].

In the silicon industry, photolithography is a key technology that has successfully reduced the scale of the pattern to produce features with high-resolution in one device. In addition, this technology is also economically viable due to the capability of high-yield wafer-level production [8], [37]. However, it is difficult to microfabricate on biodegradable substrates because biodegradable polymers are extremely vulnerable to damage from organic solvents, plasma environments, thermal loading, and ultraviolet (UV) light during common microfabrication processes like photolithography, etching, and deposition. As a consequence, high surface roughness, peeling off, nonuniformity, and air bubbles inside layers cause device failure [22]. Thus, in order to fabricate biodegradable devices, conventional microfabrication techniques, such as

photolithography-based patterning, etching, and deposition, must be adopted. This is a crucial step in the development of highly miniaturized and biodegradable gadgets.

2.2 Microstamping

Soft lithography, which refers to the use of soft, elastomeric materials in pattern generation, has been related with some of the most interesting research in the microfabrication field. A high-resolution elastomeric stamp with a chemical ink that can create a self-assembled monolayer (SAM) on a target substrate is used in the earliest soft-lithographic technique, which is a type of contact printing [38]. In order to produce patterns of other materials, this monolayer can direct material deposition on or removal from the substrate. The potential of this method to create structures with dimensions that are in the submicron range while utilizing standard chemical laboratory equipment and low-cost facilities is what draws researchers' attention to it. The two stages of the soft lithography process are the creation of the elastomeric elements and their application to the patterning of features in geometries determined by the relief structure of the elements. While it is occasionally possible to use patterns created by a stamp to create a replica of that stamp, these two procedures are often very distinct from one another. The master refers to the structure from which the stamp is derived and is frequently defined by an established lithographic method. Any method that is capable of fabricating clearly defined structures of relief on a surface can be used to produce it. From a single master, several elastomeric elements can be produced, and each one can be used repeatedly throughout patterning [39]. Steps for the fabrication of PDMS stamp for patterning poly(urethane) are given as an example in Fig. 2.2. Here in this method, a Si wafer is photolithographically patterned with a thin coating of photoresist. A prepolymer that can be cured by light or heat is cast against this master to create elastomeric components. For this purpose, the elastomer poly(dimethylsiloxane) (PDMS) is frequently utilized. This fabrication sequence offers extremely high precision when using optimal materials and chemicals, for instance, the molecular structure of the polymers, their conformation, and the degree of crosslinking can play significant roles [39].

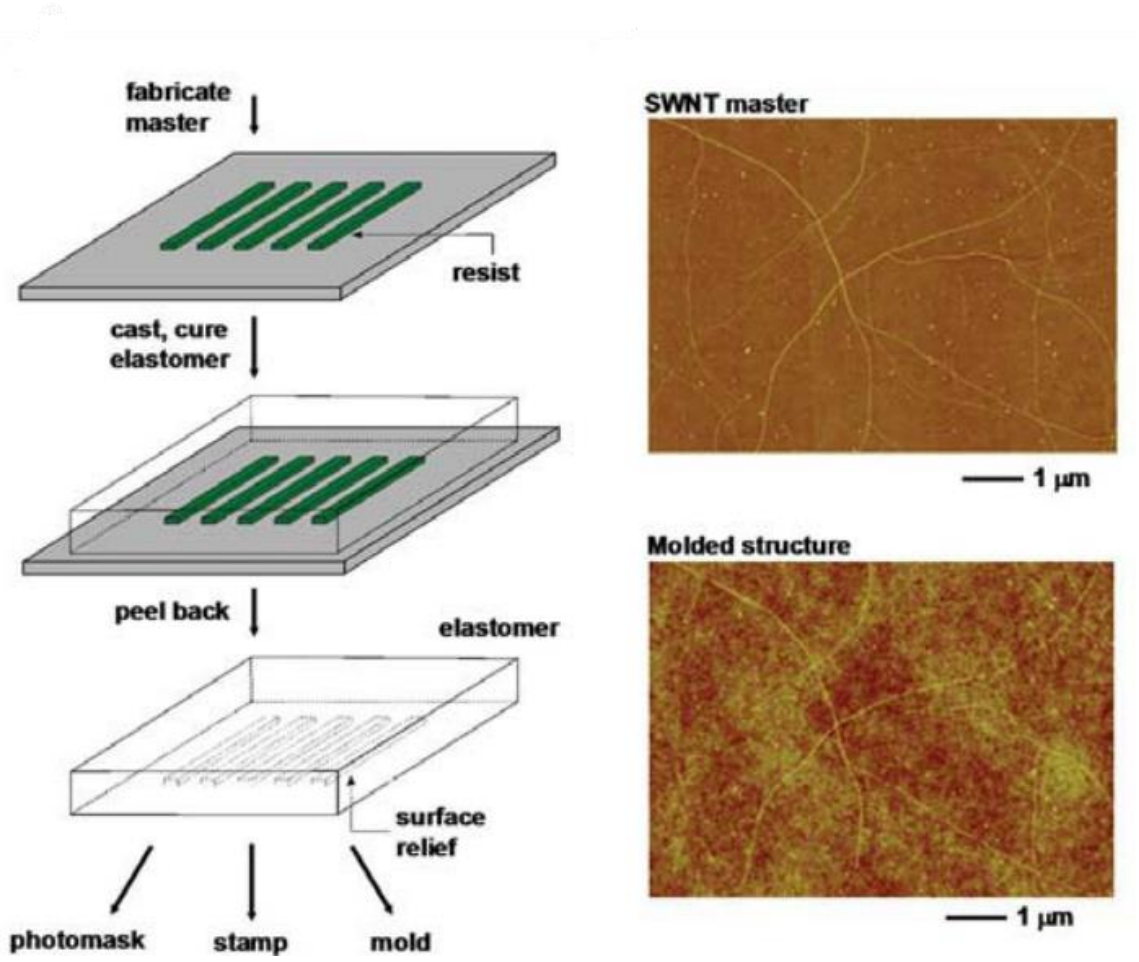

Figure 2.2: Steps for the fabrication of PDMS stamp using soft lithography (on the left) and atomic force micrographs (AFM) result of the master having submonolayer of single-walled carbon nanotubes (SWNTs) with on SiO_2/Si substrate (on the right top) and molded PU formed by soft lithography using PDMS, fabricated from SWNT master. Taken with permission from [39].

As mentioned earlier, a single master can be produced and used repeatedly to fabricate the stamps, which can be used several times for patterning. The advantages of the soft lithography method are that the fabricated stamps can be used several times without being damaged, so it is an extremely time saving and low-cost method. In addition to this, the usage of polymers for patterning using the fabricated stamps are already mentioned in the literature, so soft lithography method is already a more polymer-compatible method compared to the other methods which can damage the polymer considering the properties of biodegradable polymers. Since it is difficult to microfabricate on biodegradable substrates because biodegradable polymers are extremely vulnerable to damage from organic solvents, plasma environments, thermal

loading, and ultraviolet (UV) light, these parameters should again be considered during the patterning of the biodegradable substrate with the fabricated stamp. Examples for the fabrication of stamps and the patterning methods of biodegradable substrate using these stamps will be given in the results chapter. Since mostly stamping term will be mentioned instead of the general term “soft lithography”, this method will be named as microstamping throughout this thesis.

2.3 Laser Ablation

Laser ablation method is used to alter the material's shape or appearance using laser energy. The ability to quickly change designs, fabricate products without the need for retooling, and raise the quality of the final products are just a few benefits of the laser ablation technique. The ability to process a variety of materials is another benefit. Metals like aluminum (Al), iron (Fe), stainless steel, and titanium (Ti) are among the metals that can be used, together with non-metals including ceramics, composites, plastics/polymers, and even adhesives [40].

In laser ablation, the substance is removed through physical means. The material is totally removed from the top to the bottom surface or only partially, depending on the desired depth. Laser cutting, laser engraving, and laser drilling all involve the ablation of material. In addition, the effects created when a material interacts with laser radiation in laser ablation method depend heavily on the substance's chemical composition, absorption properties, and wavelength, as well as the laser's power level [40]. Typical laser ablation methods, such as laser drilling, cutting, and engraving for the patterning of a substrate can be seen from Fig. 2.3.

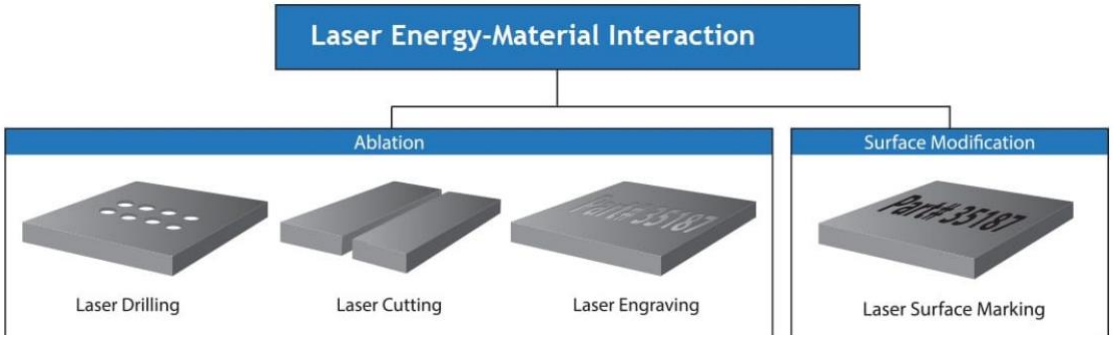

Figure 2.3: Summary of laser ablation methods for the patterning of a substrate. Taken with permission from[59].

By etching metal on a polymeric substrate, laser ablation can also be used for producing patterned structures [41]. By raising the substrate temperature over the glass transition temperature (T_g), the heat generated during the ablation damages the heat-sensitive substrates, which causes deformation or the creation of crack on the substrate [42]. Even though this does not cause any problem for some of the substrates, for the patterning of the biodegradable substrates, it is a very critical issue that mostly does not allow their usage in laser ablation technique. Since this is a straightforward and a much easier technique, if it can be adapted to biodegradable material patterning by eliminating the disadvantages, it would be a very useful technology.

2.4 Transfer Printing

It is possible to assemble nano- and micromaterials deterministically into functional configurations with two- and three-dimensional layouts using transfer printing. These methods provide adaptable ways to test high-performance, heterogeneously integrated functional systems, including flexible electronics, three-dimensional and/or curvilinear optoelectronics, and bio-integrated sensing and therapeutic devices, in addition to the structures and tools used in scientific research [43]. The transfer printing technique, which permits the high yield transfer of solid objects from a donor substrate to a receiver substrate, is the most effective way to conclude this assembly process. By separating the fabrication substrates from the application substrates, this approach avoids the problem of polymeric substrates being incompatible with standard fabrication technologies that have a developed, established commercial infrastructure, and it makes it easier to commercialize flexible and stretchable inorganic electronics [44]. The most popular method of transfer printing uses a soft, elastomeric stamp to enable the physical transfer of microdevices, also known as inks, in large quantities between a donor substrate and a receiver substrate [45]. The donor substrate, on which the inks are normally arranged and made releasable via wet chemical etching or dry etching (for instance, laser lift-off), is in touch with the stamp at the very beginning of the retrieval process. Wet chemical etching, for instance, produces releasable inks by etching a sacrificial layer between the inks and substrate, yet with sufficiently defined anchor structures to maintain the lithographically established spatial layouts of elements. The stamp is properly preloaded to allow for

conformal contact between the inks and the stamp, resulting in enough adhesion to remove the inks from the donor substrate. The retrieval method can be either non-selective for exact manipulation on one or more inks, or selective for accurate manipulation in a highly parallel manner, to achieve high throughput. Once the inked stamp and receiving substrate are in contact, the stamp/ink adhesion is adjusted to print inks onto the substrate. Removal of the stamp marks the end of the transfer printing process [44]. A typical transfer printing process can be seen in Fig. 2.4.

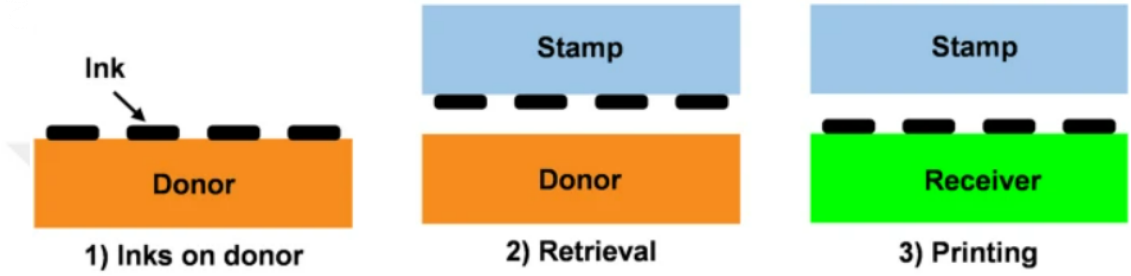

Figure 2.4: Step by step description of a conventional transfer printing method. Taken with permission from [44].

Transfer printing process can be categorized into three categories: Additive transfer, subtractive transfer, and deterministic assembly. First method, additive transfer performs well for working with a variety of organic and inorganic materials, in which a receiving substrate and an entire ink layer—or just a portion of one—that has been deposited on the surface of a stamp, transfer to one another. Solution casting and physical vapor deposition are two techniques that can be used to ink the stamp. Layers created by additive printing technologies can be used for a range of tasks, including the creation of integrated device components and the creation of etch masks for additional processing. The second method, called subtractive transfer, employs a stamp to pick and choose which portions of a blanket film to extract. This printing technique can be used to etch windows in etch masks, allowing access to the materials beneath for further processing, or to directly pattern an active layer. To facilitate the transfer, the receiver can be chemically modified, heated, or have thin intermediary polymeric adhesion-promoting layers put between the stamp and ink. This mode, in contrast to additive printing, requires robust fracture of the ink layer, which adds a new set of design considerations.

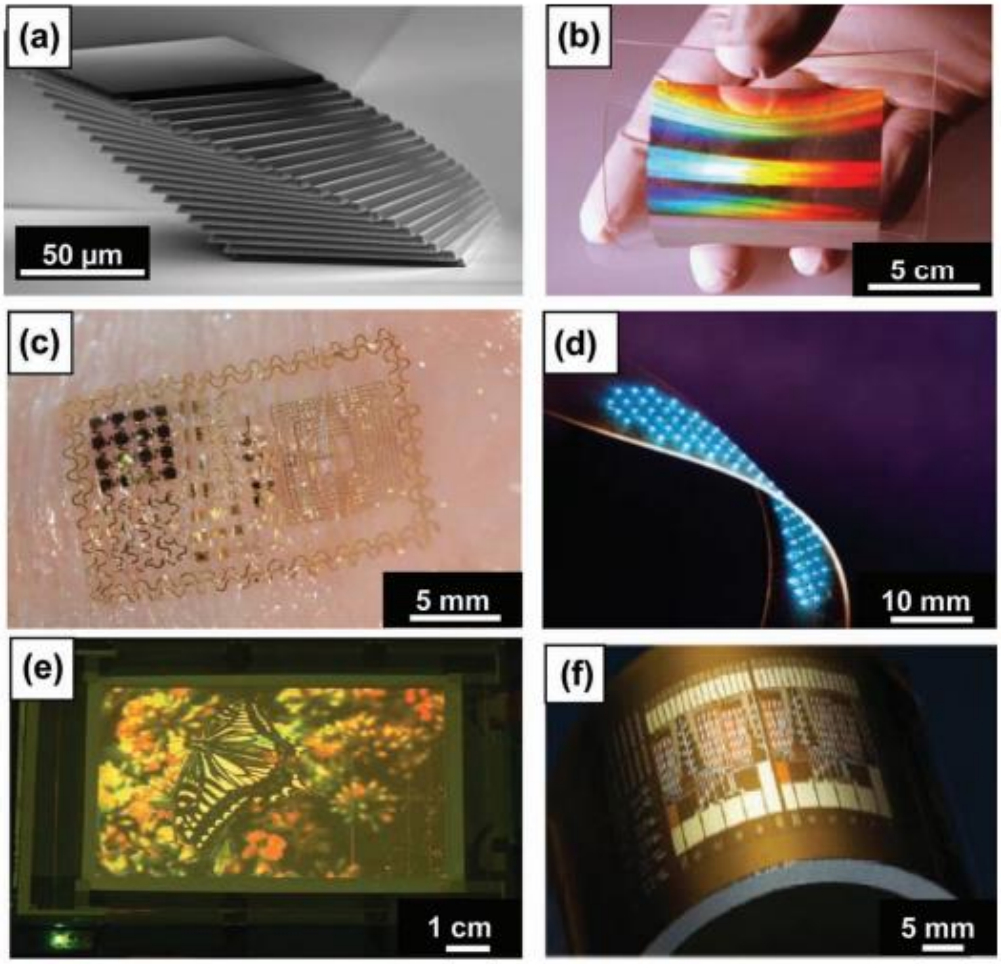

Figure 2.5: Exemplary devices fabricated using transfer printing. Taken with permission from [43].

Subtractive transfer can occasionally act as the inking phase of an additive transfer process. These technologies can produce specific structures on a donor substrate for use in deterministic assembly techniques, in addition to more conventional processing or growing operations. One of the numerous advantages of this technology is how much more material options are available for production because the inks' development and processing are separated from the stamp and the receiving substrate. These methods usually rely on dynamic, reversible adjustment of adhesion forces to the stamp as well. [43]. Exemplary devices fabricated using transfer printing method can be seen in Fig. 2.5.

To align and arrange biodegradable layers on various surfaces for making biodegradable electronic devices, transfer printing technique can also be used. Although the transfer printing method is capable of transferring parts with features as small as tens of nanometers, there are difficulties in transferring ultra-thin parts (below 200 nm) and parts with a non-sticky surface that call for the best surface preparation. The widespread

application of microfabricated biodegradable devices has also been limited by the requirement for specialized equipment in this method [22].

2.5 Inkjet Printing

Desktop printers can now reliably copy text, images, and photos on paper and several other substrates using inkjet printing, a cutting-edge technique that is currently being employed in the field of materials deposition. This interest in "maskless materials deposition" goes hand-in-hand with the development of microfabrication methods for the realization of circuits or patterns on flexible substrates, for which printing methods are crucial [46].

The two operating modes for inkjet printers are continuous and drop-on-demand (DOD). Inkjet printing in continuous mode involves pumping ink via a nozzle to create a liquid jet. By applying a periodic disturbance, which causes the jet to break up due to surface tension, uniformly spaced and sized droplets are produced. Continuous-mode graphical applications like textile printing and labeling are among the main uses of inkjet printing. Due to its lower drop size and higher placement precision, the second operating mode, drop-on-demand is the method of choice in most cases. Droplets of ink are released from a reservoir through a nozzle by an acoustic pulse and piezoelectricity or thermal energy can be used to produce this pulse. In a thermal DOD inkjet printer (also known as a bubble-jet), ink is heated locally to create a vapor bubble that expands quickly and ejects an ink droplet. The number of polymers that can be printed with thermal DOD may be limited because water is typically used as a solvent, while there are non-aqueous thermal inks available as well. On the other hand, piezoelectric DOD inkjet printing depends on the deformation of a piezoelectric material to cause a quick change in volume and afterwards produce an acoustic pulse. Piezoelectric DOD is, in theory, compatible with a range of solvents. The ink and its physical characteristics, particularly its viscosity and surface tension, are perhaps the most important aspect of inkjet printing technology. Viscosity should be appropriately low, usually less than 20 mPa.s. When too much kinetic energy is suddenly lost, no droplet is expelled. Because of this, eventual polymer solutions should be appropriately diluted. However, because inkjet printing typically involves shear rates of the order of $10^5.s^{-1}$, shear-thinning is possible. For a given pressure wave at the nozzle, the velocity and amount of fluid driven forward increase with

decreasing viscosity, generally producing lengthy tails behind the head of the drop [47]. The liquid drop that comes out of the nozzle has a spheroidal shape because of surface tension. Xylene, for example, has a surface tension of 28 $mN.m^{-1}$, while molten solder has a surface tension of 350 $mN.m^{-1}$ [48]. Additionally, because wetting the nozzle outlet face results in spray, the wetting behavior of the fluid and the nozzle material is also important [47].

Another suggested mask-free fabrication method for biodegradable electrical devices is inkjet printing. The minimal feature size is restricted, and it cannot give reproducible results for batch manufacturing because it depends on the geometrical properties and kinetics of the printer nozzle. For the production of high-resolution biodegradable sensors, the chemical composition of the printer ink must also be changed [49]. When utilizing shadow masks for microfabrication, it is difficult to get a tight fit on the substrate which involves manual work, and any gaps remained cause a short circuit [49]. Additionally, applying more than T_g causes the mask to stick to the substrate, which causes the polymeric substrate to peel off when the mask is removed [20]. In this case, inkjet printing method cannot be mentioned as the optimum method for the patterning of biodegradable devices even though there are some examples in the literature. An example from the literature for the fabrication of biodegradable capacitors and thin-film transistors (TFTs) using inkjet printing method can be found in Fig. 2.6.

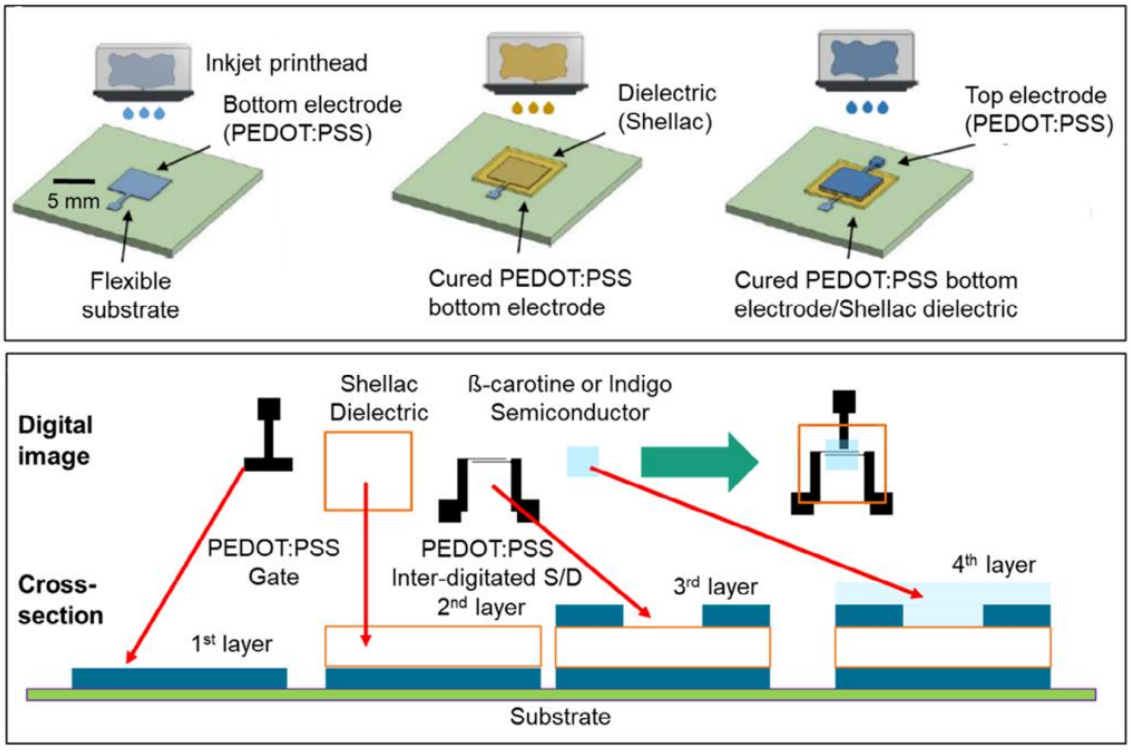

Figure 2.6: Inkjet printing method using PEDOT:PSS as conductive polymer. Parallel plate capacitor (on top) and bottom gate bottom contact (BGBC) TFT (on bottom). Taken with permission from [49].

2.6 Stencil Lithography

The principle of stencil lithography is to use several processes like deposition, etching, or ion implantation to locally alter a substrate surface while using a flux of atoms, molecules, or particles as a shadow mask. In contrast to resist processing used in traditional lithography, the stencils are mechanically stable and self-supporting, allowing them to be relocated during processing and reused multiple times [50]. The fabricated stencils can be used for multiple purposes, such as material deposition or dry etching. In the case of material deposition, without employing any resist processing, a stencil is placed in between a substrate and a source to mask the deposition of the impinging material flux. As a result, the structures that are deposited into the substrate are duplicates of the aperture patterns in the stencil [50]. A stencil is applied on the material that is intended to be etched as a hard mask for the dry etching process instead of utilizing any resist as a mask for etching. Both material deposition and dry etching using stencils will be covered throughout the results of this thesis.

Two different types of stencil lithography techniques can be found in the literature based on the characteristics of the materials. A rigid stencil mask made of Si or SiN_x is first type for stencil lithography, whereas a flexible membrane, such as PI film, PDMS, and photoresist can also be considered for stencil lithography [51]. Since rigid stencils are the most common type and will be covered throughout the thesis, the details of rigid stencils will be explained in the coming section.

2.6.1 Rigid Stencils as Masks

Silicon Nitride Membrane (SiN_x)

The development of metamaterials in recent years has made it possible to identify biomarkers at low concentrations using spectral shifts at Tera-hertz frequencies (THz). Patterning such metamaterials for point-of-care (POC) applications is becoming very common on inexpensive and disposable substrates. While paper is an excellent substrate because it is disposable and light, conventional patterning techniques, however, cannot

be used to create such microstructures on paper [51]. For this purpose, in order to pattern metamaterials on a paper substrate and enable the paper to detect glucose and urea with high sensitivity, Tao et al. used a SiN_x microstencil, which is an excellent material for stencil lithography due to its high thermal stability, mechanical strength, and chemical inertness. On a silicon wafer, a 500 nm thick SiN_x film was deposited, and then the SiN_x film was patterned using conventional surface micromachining methods. A free-standing SiNx membrane was produced by using KOH to etch the silicon wafer from the back. To create metamaterials, the SiNx microstencil was placed on top of the paper substrate, and then a thin gold layer was deposited trough the stencil [51].

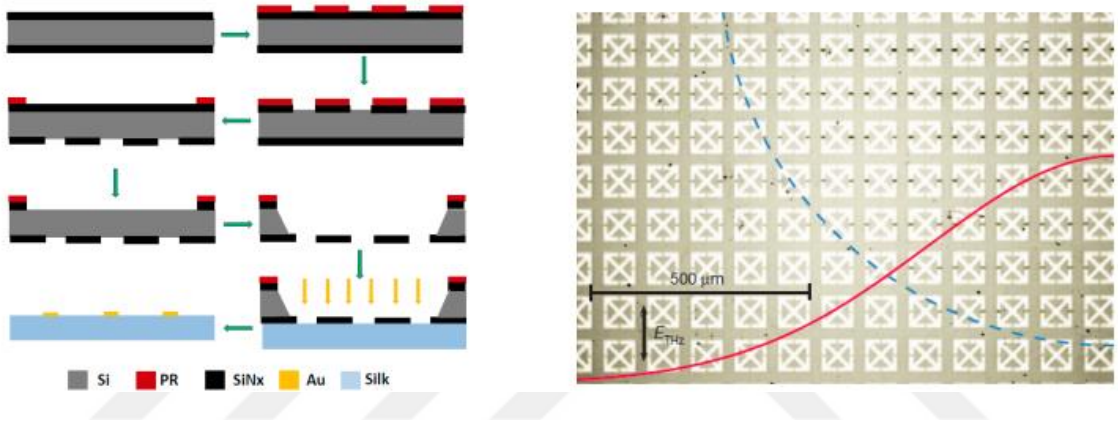

Figure 2.7: Fabrication of a SiN_x mask for a silk-based sensor (on the left) and micrograph of a metamaterials sensor fabricated by this mask (on the right). Taken with permission from [52].

The stencil lithography method utilizing a SiN_x stencil could also be used to print metamaterials onto silk composites. Silk composite is transparent, water-soluble, flexible, and biocompatible, which makes it essential for developing IMDs. Without the use of stencil lithography, it is challenging to install a biosensor on a curved surface for in situ detection [52]. An example of a metamaterials sensor fabricated by using SiN_x-based stencil lithography can be seen in Fig. 2.7.

Silicon Membrane

As rigid stencil masks, low-stress SiN_x membranes have commonly been utilized in large quantities; nevertheless, silicon membranes are gaining vast popularity. By utilizing deep reactive ion etching (DRIE), an aspect ratio of over 50:1 can be obtained on a silicon membrane. A thicker silicon stencil mask can be developed compared to a silicon nitride

mask due to the high anisotropy of silicon materials during DRIE, thus, it becomes easier to manufacture and handle the silicon membrane, which is a great advantage for the fabrication of nano structured stencils. Even if the intrinsic stress in silicon membrane is higher than that in silicon nitride, increasing the film thickness may be able to prevent cracks from developing. The second advantage is that a potassium hydroxide (KOH) solution can wet-etch a single crystalline silicon membrane. Wet etching can be carried out in an ambient surrounding, which greatly lowers the cost of the procedure. Additionally, wet etching on a single crystalline silicon enables adjustable cone angles and aperture diameters and as a result, the conventional photolithography procedure can be used to pattern sub-50-nm apertures on silicon stencils [51]. Utilizing photolithography and wet etching, Deng et al. created these pyramidal silicon nanopore arrays. First, a 4 μm by 4 μm feature size was established using photolithography, and then silicon was wet etched using KOH. Pyramidal nanopore arrays with 20-nm pore sizes were created by chemical wet etching a P-type (100) silicon wafer. The silicon stencil was then utilized to pattern the metal on the substrate [53]. The schematic of the stencil of pyramidal silicon nanopore arrays can be seen in Fig. 2.8.

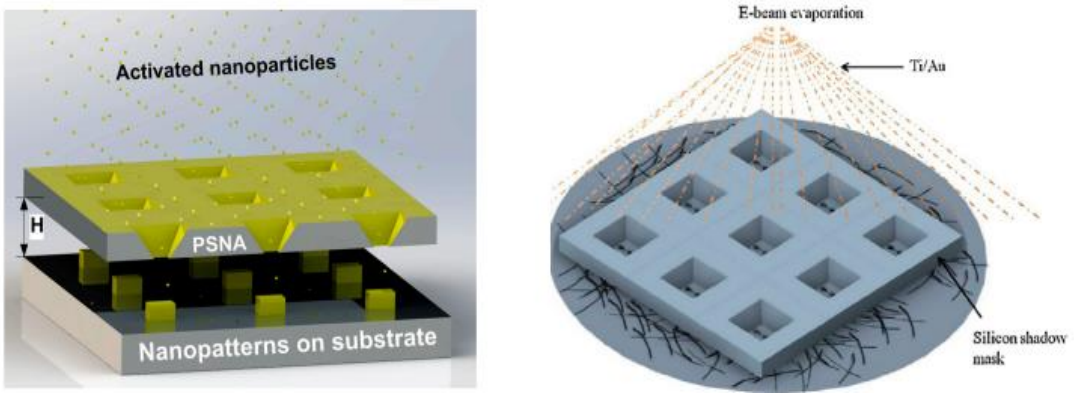

Figure 2.8: Nanostencil mask with pyramidal arrays (on the left). Taken with permission from [53]. Silicon hard mask for single-walled nanotubes (SWNTs) metallization (on the right). Taken with permission from [54].

Stability and contact resistance minimization play a critical role in the characterization of nanoelectronics, including transistors made of graphene and carbon nanotubes. By using stencil lithography, metallic connections to these nanomaterials can be patterned. Electrodes were patterned onto the surface of single-walled carbon nanotubes (SWNTs) by Agarwal et al. using a silicon stencil mask. On the target substrate, SWNTs were first applied, and then a silicon stencil mask was placed on top of the SWNTs for depositing electrode through the stencil. The electrical characteristics of

the SWNTs could be determined by measuring the resistance of the patterned electrodes after stencil lithography was used to pattern electrodes. The advantage of using this method here is that without further coating and photoresist patterning on the SWNTs, the patterning procedure can be finished with only one step [54]. A schematic of the electrode patterning on SWNTs can be seen in Fig. 2.8.

2.6.2 Advantages of Using Stencils as Masks

Avoiding Resist Processing

Since stencil lithography doesn't need a resist layer, it can be employed without the use of organic substances, solvents, energy radiation, or mechanical pressure. This makes it possible to apply stencils to substrates with chemically delicate surfaces, such self-assembled monolayers (SAMs), organic molecules, or materials that are sensitive to radiation. Additionally, it makes it possible to pattern mechanically delicate structures like cantilevers and free-standing membranes. Therefore, stencil lithography is a practical choice for patterning high-topography wafers when spin or spray coating is challenging or even impossible [50].

Simple Handling and Application

Almost anyone with access to a physical vapor deposition (PVD) tool can use the technique. By simply employing adhesive tapes or mechanical fixture chucks to secure the nanostensils on a substrate, different designs can be successfully achieved in any process, such as etching, deposition, or implantation [50].

Reusability

The stencils can be used repeatedly, enabling the cost-effective duplication of patterns with different materials onto multiple substrates. The so-called clogging of the membrane apertures can limit the stencils' capacity to be reused for deposition through nanoscale apertures. Different than deposition, clogging is not a problem for etching and ion-implantation [50].

Dynamic Stencil Lithography

During deposition, the stencils can also be shifted with respect to the substrate. Using a single mask, this mode permits the manufacturing of structures with variable thickness as well as the production of multi-material structures with various patterns. Dynamic stencil deposition, for instance, makes it possible to pattern closed loop structures like rings, which are not achievable with static stencil deposition[50].

2.6.3 Disadvantages of Using Stencils as Masks

Blurring

The structures that are deposited through stencils are larger than the apertures of the stencils because of the gap that exists between the stencil and the substrate by nature. The resolution of the deposited patterns is limited by the difference in material flux and the degree of freedom of the deposited material diffusing on the surface. The impact of blurring increases as structure size decreases. At the nanoscale, the blurring can have a size that is comparable to or even larger than the aperture size itself [50].

Clogging

If the thickness of the material that is deposited is comparable to or higher than the size of the stencil aperture, the buildup of the deposited material on the membrane and inside the apertures causes an important decrease in the aperture size. Although this effect can be exploited to produce even smaller or conical designs, it eventually has an impact on the patterns that are deposited and restricts the use of the stencils again. If the thickness deposited is substantially more than the size of the stencil aperture, the apertures might even close during a single deposition [50].

Membrane Stability

The creation of nanoapertures requires a decrease in membrane thickness because dry etching techniques are limited in the aspect ratios that can be achieved. The membranes become more fragile as a result, which can be countered by reducing their lateral size and, consequently, the patterning area. The thickness of the membrane is set

by striking a balance between the size of the apertures, local membrane stability, and membrane size as a whole [50].

The aim of this thesis is to investigate possible microfabrication techniques for patterning biodegradable polymers. So, in the introduction chapter, initially, certain characteristics of biodegradable polymers that can be used in device microfabrication are discussed. Secondly, potential microfabrication techniques for patterning biodegradable substrates, including photolithography, microstamping, laser ablation, transfer printing, inkjet printing, and stencil lithography, are illustrated by discussing the advantages and disadvantages of each technique. In the coming chapter, the use of deep reactive-ion etching (DRIE)-based Si-stencils for patterning biodegradable substrates and additional uses for the fabricated DRIE-based Si-stencils will be examined. This thesis will concentrate on outlining the benefits and drawbacks of various microfabrication techniques for the patterning of biodegradable substrates.

Chapter 3:
DRIE-BASED SI-STENCIL FOR THE PATTERNING OF BIODEGRADABLE SUBSTRATE

3.1 DRIE-Overview

3.1.1 Dry Etching Techniques

In general, the term "dry etching" refers to a variety of techniques, including plasma etching, reactive ion etching (RIE), and ion milling. The process pressure used in the etch chamber while etching is a significant distinguishing factor among these various methods. Plasma etching is carried out at process pressures that are relatively higher (10^{-1} to 10^{2} torr). Before colliding with the substrate, the plasma's constituents travel along mean free pathways that are quite short. This type of dry etching is more isotropic in nature since the etching species contact the substrate at a variety of angles because of these collisions. As a result, rather than being predominantly influenced by physical processes, plasma etching is mainly determined by chemical reactions among the plasma species and the material that is exposed to be etched. Plasma etching is similar to wet etching in that it lacks directionality but is more material selective. Ion milling is a type of dry etching that solely relies on mechanical plasma ion bombardment of the substrate surface, with no chemical reactions involved. The mean free route of the species is much longer than the reaction chamber, where process pressures are 10^{-3} torr or lower. The plasma species can sustain greater energy levels because they do not collide, which allows them to transfer that kinetic energy to the surface atoms when they strike the substrate. The etching technique used in ion milling has a very low lateral etch rate and is highly anisotropic. In addition, ion milling is a non-selective method. As a result, it is ineffective for etching materials deeply (more than a few microns). Even so, it's routinely employed to etch substances that can't be engraved in any other way. RIE combines the advantages of the plasma etching and ion milling methods. In RIE, the atoms of the substrate surface receive sufficient kinetic energy from impacting plasma species to begin the etching process. Substrate atoms then react chemically with the responding species and desorb from the

surface as reaction byproducts. As a result, RIE delivers better anisotropy of the etched features than ion milling while also being more material specific [55].

3.1.2 Inductively Coupled Plasma (ICP) RIE Etching

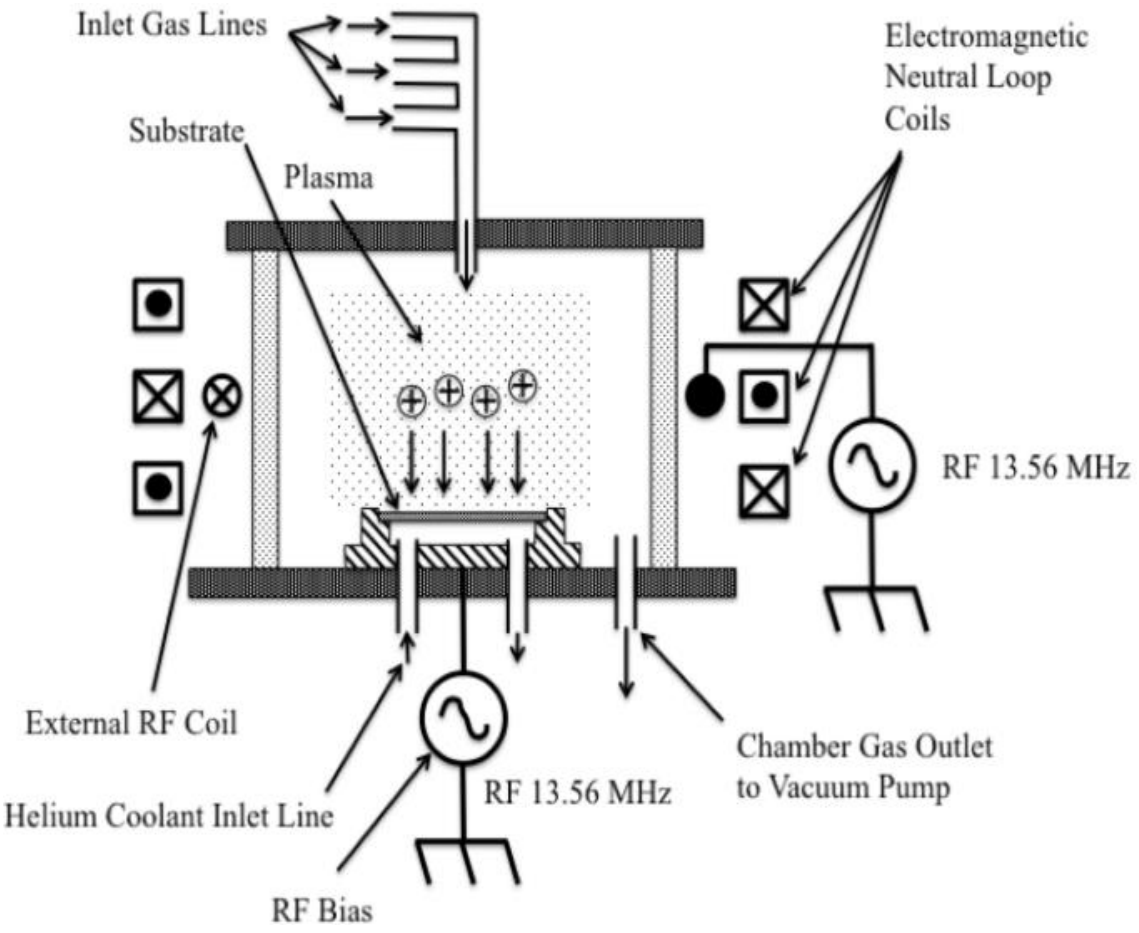

Figure 3.1: Illustration of ICP-RIE system. RF generators to create and sustain the plasma and to bias the reactants to the substrate can be seen. Taken with permission from [60].

Although RIE is frequently used in microfabrication, it has not proved effective for deep, high-aspect-ratio silicon etching because the depths of the etchants are typically only a few microns. Bulk micromachining needs etching depths of several hundred microns, including 500 microns or more entirely through the substrate, as well as high aspect ratios. Another kind of RIE configuration that is more appropriate for deeper and high-aspect-ratio etching is the inductively coupled plasma (ICP) etch setup. A separate RF generator employs an electrical field to direct the reactants toward the substrate and

generate a highly anisotropic etch result, while the plasma in the ICP etch arrangement is formed using an RF-powered magnetic field. The ICP configuration has the benefit of producing very high plasma concentrations at low operating pressures, enabling an elevated etch rate as well as acquiring a more anisotropic etch profile because the reactants are biased via the bottom electrode, which is disconnected from the field sustaining the plasma [55]. One version of an ICP etch system is shown in Fig. 3.1.

3.1.3 Cryogenic DRIE

Fluorine radicals generated from sulfur hexafluoride gas (SF_6) in the plasma discharge are used as the etching species in cryogenic deep and high-aspect-ratio plasma etching. When oxygen gas (O_2) is injected into the process chamber, oxygen radicals are produced. These radicals react with the exposed silicon surfaces to oxidize them, creating a thin-film coating of silicon oxide that protects the surfaces from the fluorine radicals' attack. The useful process window may also be increased by using an additional process gas, such as trifluoromethane (CHF_3). Importantly, liquid nitrogen is used to chill the substrate electrode during cryogenic etching, which is carried out at temperatures around 173 K. By doing this, the quantity of oxygen needed to achieve passivation and anisotropic etching while preserving a suitable etch rate and mask selectivity is reduced to a few percent of the overall gas flow. The bottoms of the features are subjected to an intense ion bombardment, which selectively eliminates the passivation there and allows the etch to go deeper into the substrate. Cryogenic etching makes it challenging to employ photoresist masking layers since the resist is a polymer and may crack at low temperatures. Certain resists with special treatments, though, might still be useful [55]. Hard masks made of silicon dioxide are more frequently utilized. Mask selectivity for a silicon dioxide masking layer is typically 100 to 1 with typical cryogenic etching rates of 4 to 5 um per minute [56]. The low process temperature is the primary drawback of cryogenic etching. The substrate's low temperature draws particles and contaminants into the process chamber, where they can adhere to the surface and cause micro-masking effects like etching grass. Since the sidewalls of the etched features can be optically smooth and there is no scalloping, cryogenic dry etching does have an advantage over

cyclical DRIE. Since sidewall smoothness is frequently important in optical and photonic applications, cryogenic etching is mainly employed in these fields [55].

3.1.4 Bosch DRIE

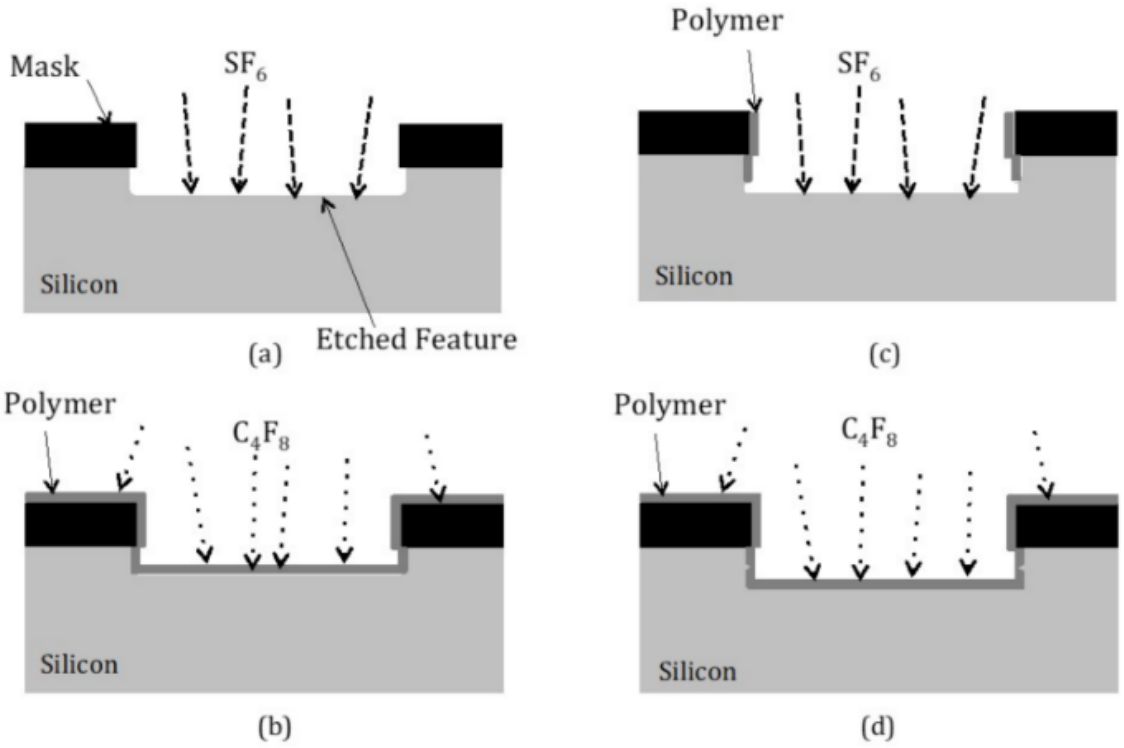

Figure 3.2: An illustration of the Bosch process for Si etch. a) fluorine-based reactive species are produced to etch the silicon with SF_6. b) SF_6 gas turns off and C_4F_8 turns on. c) C_4F_8 is turned off, SF_6 is turned back on. d) SF_6 is turned off and the polymerization gas C_4F_8 is turned on again. Taken with permission from [55].

Continuous passivation, which is truly only feasible at very low temperatures, is used in the cryogenic DRIE method for silicon etching. Although deep and high aspect-ratio etches can be made on silicon using this method, the method is susceptible to micro-masking effects. This is due to the requirement to balance the creation of silicon oxides as passivation layers, which require high ion energies to remove, with the demand to eliminate these passivation layers from the trench bottoms of the features being etched. The increased ion energies not only decrease mask selectivity but are also susceptible to micro-masking. The Bosch process, a variant DRIE method, divides the passivation and etching processes into two distinct cycles. This makes it possible to individually control the process gases for every cycle. Additionally, the silicon oxide passivation used in

cryogenic etching is replaced by polytetrafluoroethylene (PTFE), also known as Teflon, which is less brittle and takes less ion energy to remove from surfaces during the etch cycle. In the Bosch process, etch is a cyclical dry plasma technology that switches in between depositing an etch-resistant polymer layer on the sidewalls in one cycle and employing high-density plasma to etch silicon in the other cycle. While the sidewalls are coated with an etch-resistant passivation polymer layer using a C_4F_8 chemistry, the silicon is etched using an SF_6 chemistry. A typical example of DRIE Bosch process can be seen in Fig. 3.2.

Consecutive generations of DRIE systems utilizing the Bosch process have significantly boosted the silicon etching rate, with the most current generations of the Bosch process etch systems reaching 20 to 25 microns or more per minute. Reduced cycle times in more recent DRIE system versions have also enhanced the gas switching characteristics. The scalloping effects on the trench sidewalls have decreased as a result [55].

The Bosch technique for DRIE etching frequently employs photoresist and silicon dioxide as the masking layer. A rather thick photoresist mask layer will be necessary for a thorough wafer etch. The aspect ratio of the etch can reach a maximum of 50 to 1 with process optimization to the features being etched, although in practice it typically falls between 15 to 1 and 20 to 1 [56], [57]. Due to loading effects in the system, recipe of the process for DRIE may need to be modified based on the amount of exposed silicon, with larger exposed portions etching at a significantly higher rate than smaller exposed areas. In order to achieve good results, the etch should be characterized and tuned for the precise mask feature and depth [55].

For deep, high-aspect-ratio silicon etching utilizing the Bosch DRIE process, there are several general guidelines that are applicable. In general, and especially for deep, high aspect-ratio features, the etching rate has an inclination to decrease with depth. This is thought to be a result of the trench bottoms being accessible to a lower level of ion bombardment. As a result, the process essentially moves to more passivation than it did previously in the etching process. If the passivation eventually entirely replaces the etching, the etching will eventually come to an end [55], so the optimization of the DRIE recipe is crucial for an efficient deep etching process.

The etch rates for DRIE etching have improved to the point where they are adequate for production. DRIE is now often utilized for bulk micromachining of single-crystal

silicon for a variety of applications, including inertia sensors, pressure sensors, microphones, resonators, and microfluidics [55].

3.2 Fabrication of DRIE-Based Si Stencil

In order to pattern PLA biodegradable substrate, another alternative that can be used is a hard mask. This hard mask should be resistant to plasma environment that is used for patterning (etching) the biodegradable substrate and it should be used effectively multiple times without the requirement of repetitively fabricating the hard mask. For this purpose, a Si stencil was fabricated using DRIE Bosch process. Details of the fabrication procedure and the different usage purposes of the fabricated Si stencils are explained in the coming sections.

3.2.1 Back Side Patterning and DRIE Etching for the Fabrication of the Si Stencil

In order to prepare a Si stencil for the patterning of biodegradable substrate, 2x2 cm Si chips were prepared in a way that the pattern would be much smaller than the chip size so that the handling during DRIE etching can be easier. Firstly, the back side of the chip (unpolished side) was cleaned, patterned, and then etched in order to obtain a thinner mask for a more efficient patterning of the biodegradable substrate. For this purpose, HMDS treatment was done using a HMDS oven (Suss MicroTec VP8 Vapor Primer) for a better resist coating, then the positive photoresist AZ5214E (Microchemicals) was spin-coated at 5000 rpm for 90 s and later baked at 110°C for 55 s on the back side of the 2x2 cm Si chips. Patterns were defined through UV lithography (μMLA 100, Heidelberg Instruments), followed by the development using AZ 726 MIF developer (Microchemicals) for 60 s. Later, oxygen-plasma treatment (SI 500, Sentech Instruments) was done for 60 s to clean excess resist from the developed regions. After that, 100 nm Ni as the mask for DRIE etching was deposited using e-beam evaporator (KJL PVD 200 Pro Line), followed by a lift-off process using acetone to obtain 6x6 mm square back pattern. An important parameter to consider here is that the deposition of the Ni mask for DRIE etching should not be less than 100 nm as the mask removes during the DRIE

etching due to the used gases. A schematic showing the back side patterning and DRIE etching of the Si stencil can be seen in Fig. 3.3a.

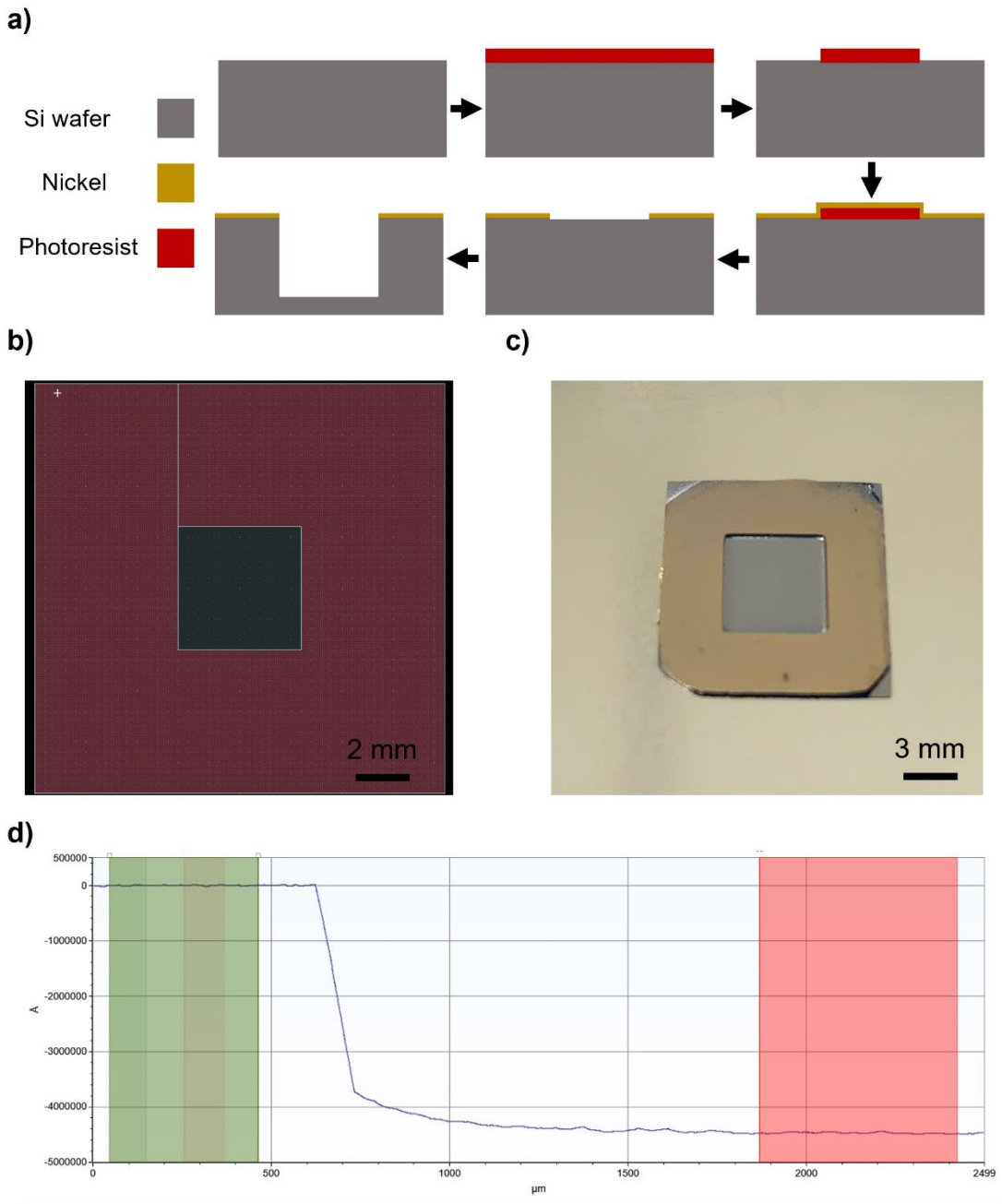

Figure 3.3: a) Schematic showing the back side patterning and DRIE etching of the Si stencil. b) Design used for exposure. c) Image of the patterned and etched 2x2 mm square (back side of the Si stencil). d) Dektak measurement of 12x15 cycles etched back side of the stencil, with a final etching depth of 440 µm. The data used in this figure was generated by Elif Yaren Özüaçıksöz and Seyed Mohammadjavad Bathaei with joint efforts under the supervision of Assist. Prof. Serap Aksu Ramazanoğlu.

Following the patterning of the back side of the stencil, DRIE (Bosch process) etching of the back side was done using ICP-RIE Silicon DRIE tool (Sentech SI 500 C with Cryogenic and Bosch process capability). All the etching experiments were done when the chiller was at -20°C, using a recipe with 240 sccm SF_6, 20 sccm O_2, and 150 sccm C_4F_8 gas flows. Firstly, 2x2 cm 6x6 mm square patterned chips were placed with a carrier wafer inside the DRIE tool. After that, the above mentioned DRIE recipe was chosen and applied for 15 cycles. The etching was continued by entering 15 cycles at once until an etching depth of 440 μm was obtained. During the DRIE etching, the etching depth was checked repetitively after several 15 cycles using Dektak profilometer for obtaining a final 440 μm etching depth. An important parameter to consider here is that the DRIE etching cycles should be kept at 15 cycles max. at a time in order to control the increase in the temperature to not to damage the patterned structures and the Ni mask. Once 440 μm etching depth was obtained (after etching 12x15 cycles), the back etching of the Si stencil was stopped. The image of the patterned and etched 2x2 mm square and the final dektak measurement of 12x15 cycles (440 μm) etched back side of the Si stencil can be seen in Fig. 3.3c and Fig. 3.3d, respectively.

3.2.2 Top Side Patterning and DRIE Etching for the Fabrication of the Si Stencil

After patterning and etching the back side of the Si stencil to 440 μm depth 6x6 mm square, the top side of the Si stencil should also be patterned and etched in order to prepare the final version of the Si stencil for the patterning of biodegradable substrate. For this purpose, firstly, the top side of the chip (polished side) was cleaned, patterned, and then etched in order to obtain the final Si stencil. For this purpose, HMDS treatment was done using a HMDS oven (Suss MicroTec VP8 Vapor Primer) for a better resist coating, then the positive photoresist AZ5214E (Microchemicals) was spin-coated at 5000 rpm for 90 s and later baked at 110°C for 55 s on the top side of the 2x2 cm Si chips. Patterns were defined through UV lithography (μMLA 100, Heidelberg Instruments), followed by the development using AZ 726 MIF developer (Microchemicals) for 60 s. Later, oxygen-plasma treatment (SI 500, Sentech Instruments) was done for 60 s to clean excess resist from the developed regions. After that, 100 nm Ni as the mask for DRIE etching was deposited using e-beam evaporator (KJL PVD 200 Pro Line), followed by a lift-off

process using acetone to obtain the main stencil pattern (circles having 50 μm diameter, 150 μm center to center distance, and a total size of 3x3 mm). An important parameter to consider here was that since the back side of the stencil was etched, it became more fragile, so it was important to be careful while handling the stencil. A schematic showing the top side patterning and DRIE etching of the Si stencil can be seen in Fig. 3.4a.

Following the patterning of the top side of the stencil, DRIE (Bosch process) etching of the top side was done using ICP-RIE Silicon DRIE tool (Sentech SI 500 C with Cryogenic and Bosch process capability). All the etching experiments were done when the chiller was at -20°C, using a recipe with 240 sccm SF_6, 20 sccm O_2, and 150 sccm C_4F_8 gas flows. Firstly, the chips were placed with a carrier wafer inside the DRIE tool. After that, the above mentioned DRIE recipe was chosen and applied for 10 cycles. In total, 2x10 cycles were applied and no more DRIE was done in order not to damage the stencil pattern. The image of the patterned and etched circles having 50 μm diameter, 150 μm center to center distance and the confocal results of 2x10 cycles etched top side of the stencil before the complete etching (with an etching depth of 24 μm from top) can be seen in Fig. 3.4c and Fig. 3.4d, respectively.

In order to etch the Si completely, the stencil was again etched from the back side square until the patterns were open. For this purpose, the same DRIE recipe was used, and the etching was done by 5 cycles 5 cycles until there were some visible openings. When there were some openings, then the DRIE was done by 1 cycle 1 cycle in order not to damage the stencil by thinning it too much. This procedure was continued until most of the patterns were ready to use and after each cycle, the stencil was checked by using an optical microscope. At this point, most of the circular patterns were visible but there were some visible remaining on some of the etched parts. An important fact to consider during the DRIE was that the etching of the pattern was not even, so even when some of the patterns were completely etched, some of them were not fully ready to use on the biodegradable substrate. In order to obtain even and clean openings on the Si stencil, following the DRIE, 15 minutes ICP-RIE Si-soft etching (SENTECH ICP-RIE plasma etcher SI 500) was done. After this final step, the Si stencil was ready to use for the patterning of the biodegradable substrate.

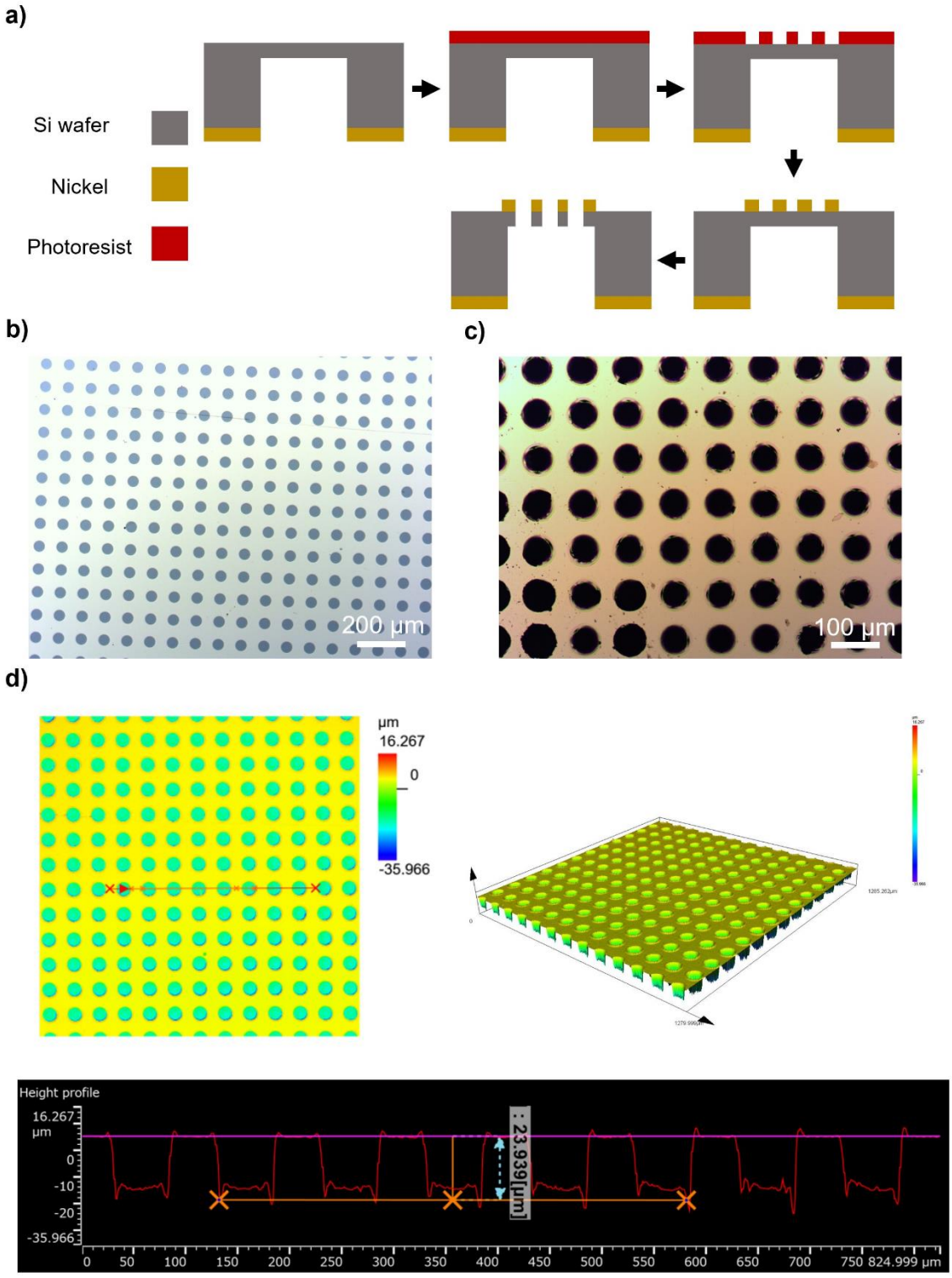

Figure 3.4: a) Schematic showing the top side patterning and DRIE etching of the Si stencil. b) Design used for exposure. c) Image of the patterned and etched circles having 50 µm diameter, 150 µm center to center distance (top side of the Si stencil). d) Confocal results of 2x10 cycles etched top side of the stencil before the complete etching, with an etching depth of 24 µm from top. The illustration used in part a was generated by Elif Yaren Özüaçıksöz and Seyed Mohammadjavad Bathaei with joint efforts under the supervision of Assist. Prof. Serap Aksu Ramazanoğlu.

3.3 Patterning of Biodegradable Substrate Using DRIE-Based Si Stencil

For the patterning of the biodegradable substrate using the fabricated Si stencil, PLA biopolymer solution was prepared and used throughout the experiments. For this purpose, 15 wt.% PLA solution was prepared by dissolving 1.5 gr PLA granules in 10 mL chloroform (Sigma-Aldrich) and mixing for 3 hours. After PLA solution preparation, the glass wafer was cut 2.5 cm x 2.5 cm and cleaned with acetone (Sigma-Aldrich) and isopropyl alcohol (IPA) (Sigma-Aldrich), respectively followed by N_2 flush. After cleaning, 40 nm chromium (Cr) was deposited on the glass substrate using metal sputter (KJL PVD 75) as the adhesion layer for PLA film. After Cr deposition, the first PLA layer

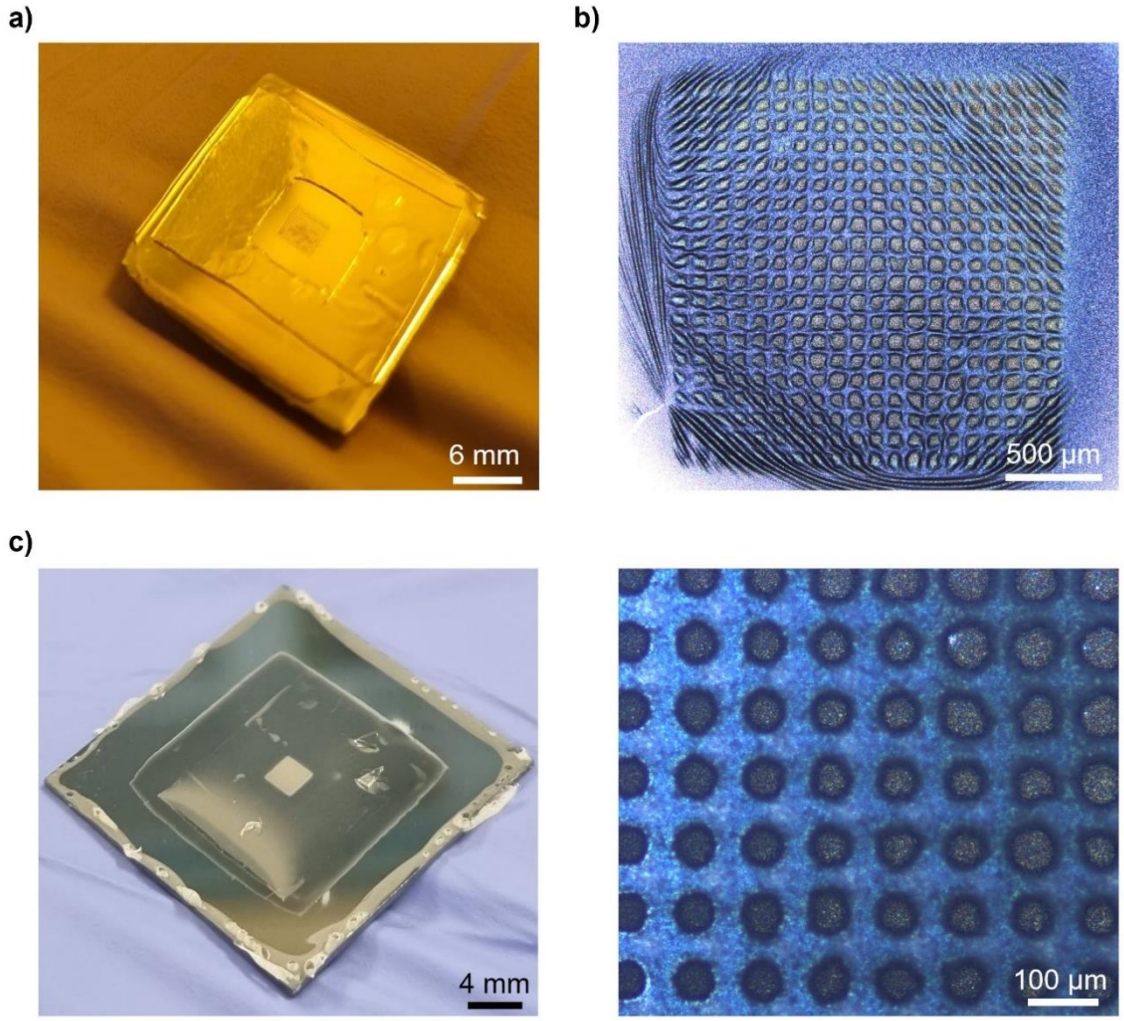

Figure 3.5: a) Image of the PDMS sheet on the Si stencil that was used to prevent the attachment of the Si stencil to PLA substrate. b) Microscope image showing the effect of longtime O_2 plasma on PLA substrate. c) Microscope images showing the patterning of PLA biodegradable polymer after etching 10x2 min.

was spin-coated using a spin-coater at 1200 rpm for 60 s and baked at 70 °C for 15 min [22]. In order to prevent the attachment of the Si stencil to PLA substrate (and to further prevent the breakage of the Si stencil due to this reason), a Polydimethylsiloxane (PDMS) sheet was used on the top side of the stencil where it was placed on the PLA substrate. The image showing the PDMS sheet on the Si stencil can be seen in Fig. 3.5a.

In order to pattern PLA substrate, dry-etching (SENTECH ICP-RIE plasma etcher SI 500) method was used by applying O_2 gas. Etching trials were done repeatedly to find the etching rate of PLA substrate. During this time, it is found that more than 2 min. of continuous application of O_2 severely damages PLA biodegradable film, so the etching

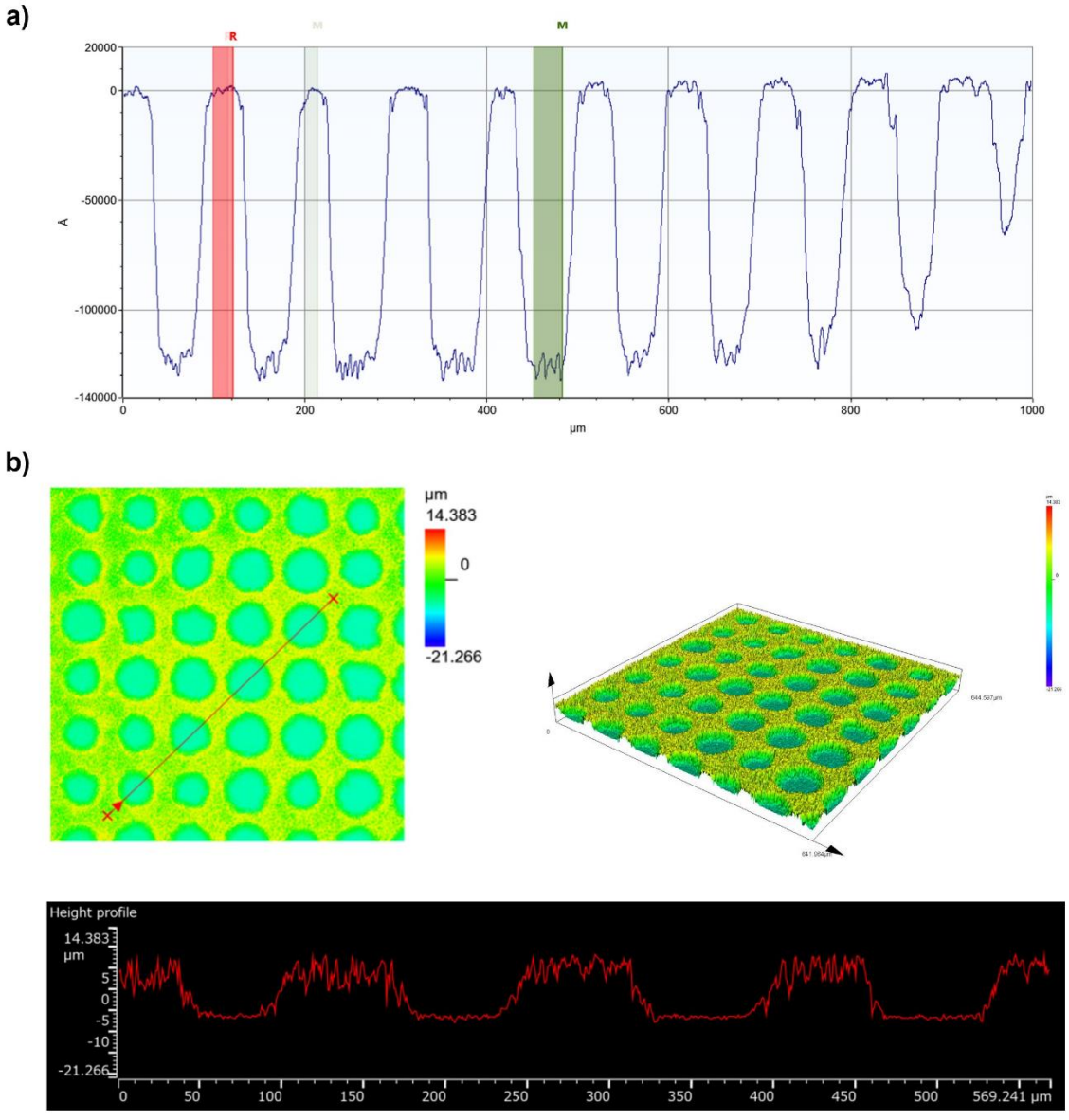

Figure 3.6: a) Dektak measurement of PLA substrate after etching for 10x2 min. Etching depth was found as 12.61 μm b) Confocal results of PLA substrate after etching for 10x2 min.

of PLA substrate was done max. 2 min. continuously (e.g. for etching 20 min., 2 min. etching was repeated for 10 times). The effect of the longtime O_2 plasma on PLA substrate can be seen in Fig. 3.5b.

After the etching depth optimization, the etching rate of PLA substrate using Si stencil was found to be 0.63 μm/min. Microscope images showing the patterning of PLA biodegradable polymer can be seen in Fig. 3.5c. Dektak and confocal results showing the depth after 10x2 min. etching (12.61 μm) can be seen in Fig. 3.6a and Fig. 3.6b, respectively.

3.4 Other Applications of DRIE-Based Si Stencil

3.4.1 DRIE-Based Si Stencil for the Fabrication of Embedded Electrodes inside a Biodegradable Substrate

By using the same protocol, a Si-stencil, having a resistor pattern was fabricated as explained in previous section. By utilizing this stencil, it is possible to embed (place) the electrodes inside the biodegradable substrate, rather than patterning it on the substrate. In this way, the electrodes will be placed inside the biodegradable substrate and while acting as an electrode for sensing applications, the sensitive metal electrode lines will also be protected from any effect that may come from outside. In addition to this, later by placing another dielectric layer (e.g., another PLA layer) on top of the embedded capacitor, the sensitivity of the capacitor can also be increased, and this will result in a more sensitive sensing. For this reason, embedding electrodes using the methods that were explained throughout this thesis can find critical applications. In order to embed Mo electrode inside PLA biodegradable polymer, firstly, the fabricated resistor Si stencil was placed on top of the PLA substrate and dry-etched using SENTECH ICP-RIE plasma etcher SI 500 as explained in section 3.3 Patterning of Biodegradable Substrate Using DRIE-Based Si Stencil. After that, without moving the Si stencil from PLA substrate, the etched substrate was directly placed on e-beam evaporator for Mo deposition (KJL PVD 200 Pro Line). 60 nm of Mo deposition was done through the Si stencil on the etched parts of the PLA

for embedding Mo electrode inside PLA. Fabricated embedded electrodes can be seen in Fig. 3.7.

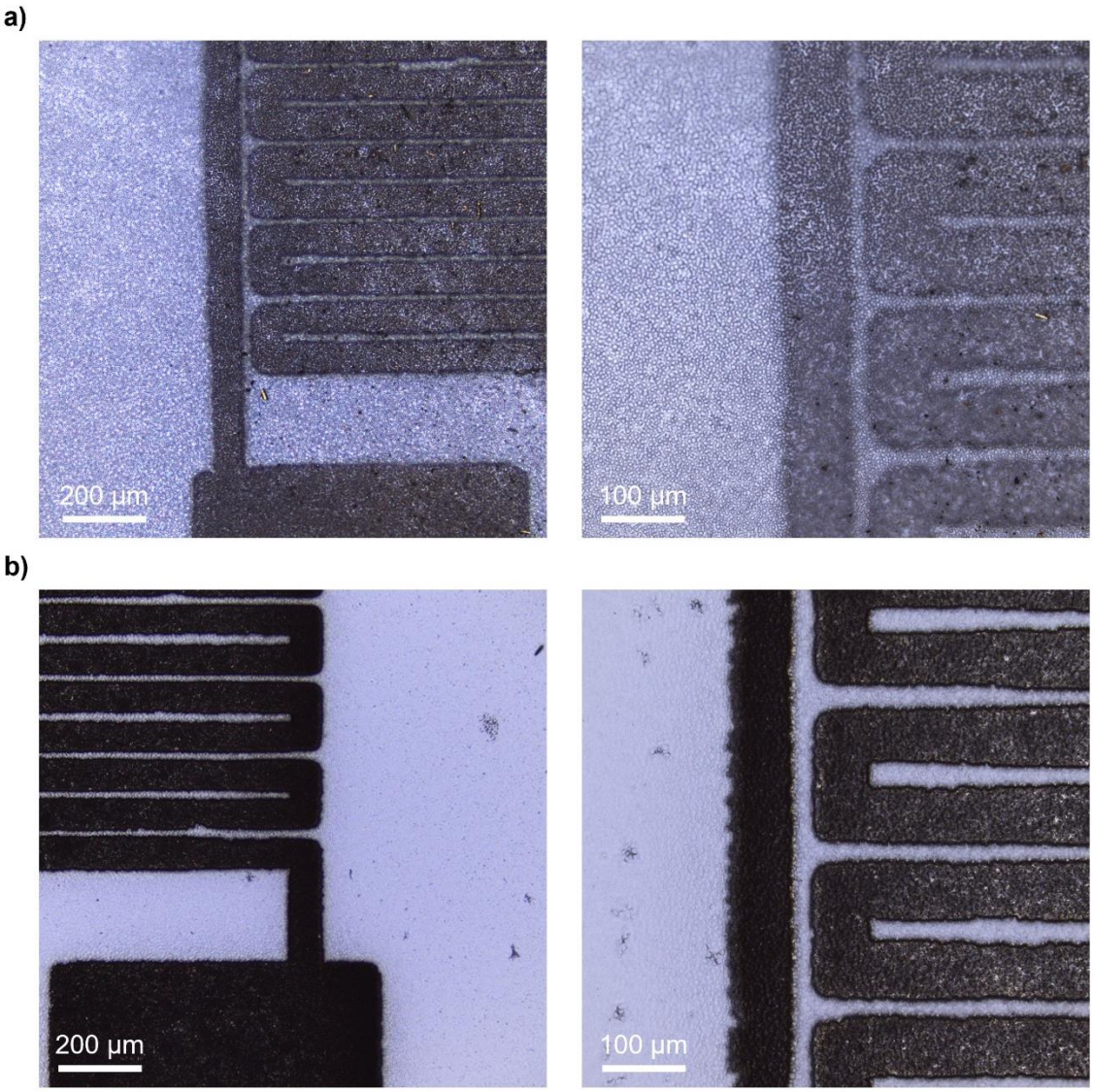

Figure 3.7: a) Microscope images of 3x2 min. ICP-RIE etched PLA substrate using resistor Si Stencil. b) Microscope images of 60 nm Mo deposited PLA substrate on the etched resistor pattern.

After embedding the electrodes, the resistance measurement was done to compare the resistance of the electrodes when they were deposited on top and when they were embedded inside the PLA substrate. While the average resistance was 796.45 Ω when the electrodes were on top of PLA substrate, the average resistance was measured as 2.0297 kΩ when the electrodes were embedded inside the PLA substrate. The resistance increase is thought to be due to the roughness of the PLA that also affects the Mo electrode. The

increased roughness in this area was due to the etching, and since the metal was directly deposited to this area, the electrodes had more cracks, thus the resistance was measured higher. The dektak profilometer result after embedding the electrodes and the electrical measurement setup can be seen in Fig. 3.8.

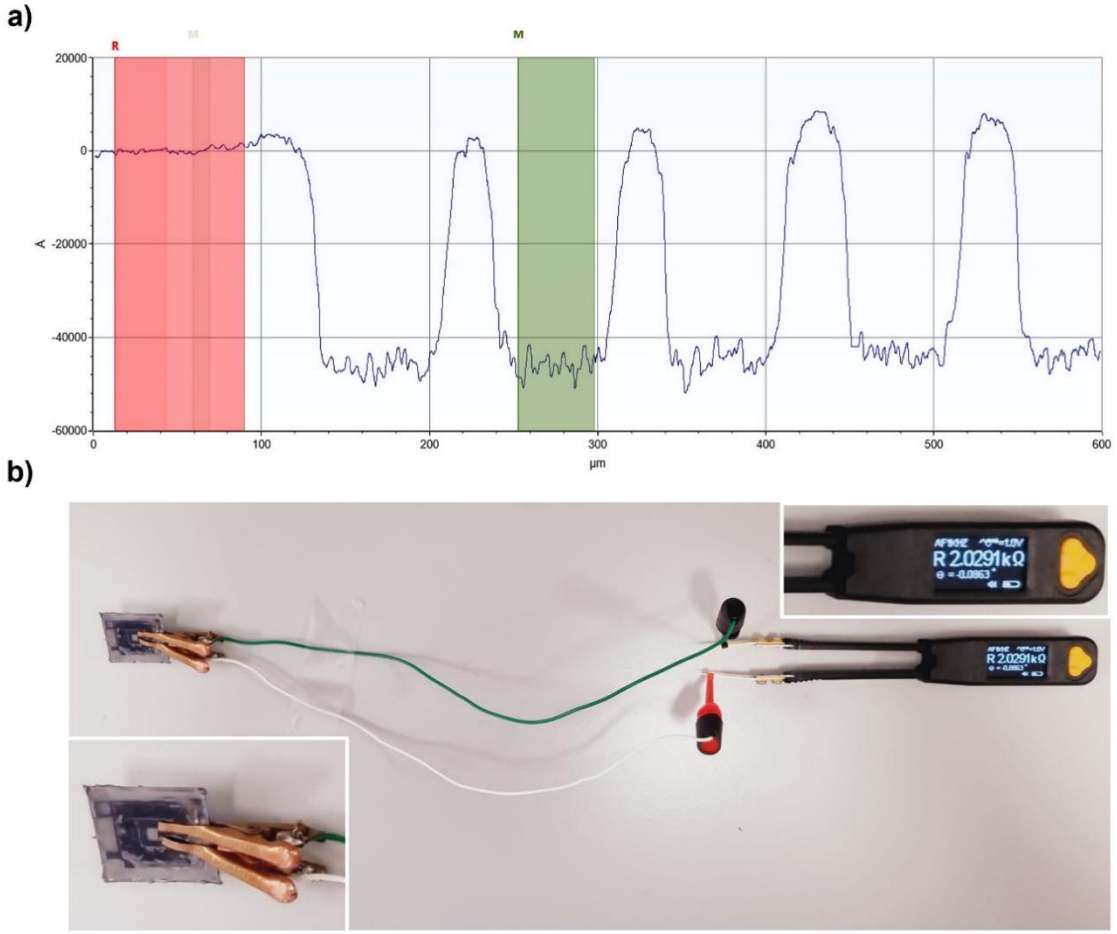

Figure 3.8: a) Dektak measurement of 3x2 min. ICP-RIE etched and 60 nm Mo deposited PLA substrate using resistor Si Stencil. The etching depth was found as 4.62 µm after embedding the electrode. b) Image showing the electrical measurement setup. The average resistance was found as 2.0297 kΩ.

Chapter 4:
CONCLUSION

Biodegradable implantable medical devices (IMDs) and recyclable, environmentally friendly membranes can be produced through microfabrication techniques that are used for patterning flexible and stretchable biodegradable substrates. The patterning of biodegradable materials has a variety of uses in both industry and medicine. In applications involving tissue engineering, it is crucial to make sure that the cells are cultivated in a way that allows them to develop, differentiate, and produce new tissues. The structures that hold the cells in place are referred to as scaffolds, and in order to create a device that functions effectively, the scaffolds must be developed with consideration for cell attachment, mechanical stability, and biocompatibility. For the purpose of building scaffolds for improved cell adhesion and localized chemical immobilization, microfabrication techniques for patterning biodegradable materials can be employed. Controllably patterning biodegradable materials can be used in drug delivery applications in addition to the cell culturing properties. In this way, the material that the medicine is encapsulated in, as well as the size and number of pores on it, regulates how much of the drug will be released. The filtering applications for material separation are another area where biodegradable material micropatterning plays a significant role. The purification of wastewater often involves the use of filters with specific-sized microholes that are created using microfabrication techniques. A key tactic for getting rid of environmental trash and promoting eco-friendly practices is switching these non-degradable filters to biodegradable ones.

In order to successfully develop micropatterned biodegradable substrates to address certain applications, throughout this thesis, different microfabrication techniques for patterning biodegradable polymers were investigated. Potential microfabrication strategies including photolithography, microstamping, laser ablation, and DRIE-based Si stencil for the patterning of biodegradable substrate were explained and the experimental results were indicated in detail throughout the chapters. In addition to the microfabrication

methods for the patterning of biodegradable substrate, different applications of the DRIE-based Si-stencils as hard masks were also mentioned.

Depending on the application purpose, according to the results shared in the previous chapters, each microfabrication strategy showed different advantages. The ability to pattern small structures efficiently and the precision to obtain the desired structures in each fabrication were listed as the two most important features of the photolithography-based patterning of biodegradable substrates. In the case of microstamping, the possibility to use the fabricated stamp repetitively and not requiring the usage of plasma for the patterning of the biodegradable substrate were the two most important advantages. In microstamping-based patterning, the pattern size was dependent completely on the tool that was used to prepare the microstamp. Because of this reason, compared to photolithography-based patterning, patterning of the small structures with a high precision was more challenging. Similar to microstamping-based patterning, in laser ablation-based patterning, the feature size and the depth of the pattern were mostly dependent on the tool that was available. On the other hand, if the laser tool could be chosen in a way that could pattern small features with a controllable depth, the laser ablation-based patterning could even become the most desired method for the patterning of a biodegradable substrate as it was a very direct method without the requirement of plasma or hard mask usage. On the other hand, since the tool used was not applicable for the applications listed in this thesis, another advantageous method, DRIE-based Si stencil, was proposed. This method consisted of a single Si stencil fabrication step using DRIE tool. Once the Si stencil was fabricated, that stencil could be used repetitively for that certain design on multiple biodegradable substrates. By changing the Si stencil design, it was not only used for patterning of the biodegradable substrate, but it was also used for patterning metal on the biodegradable substrate and even embedding electrode inside a biodegradable substrate for the sensing applications. In this way, with the DRIE-based Si stencil method proposed in this thesis, by fabricating only one Si stencil, without the requirement of photoresist or multiple additional steps, processing biodegradable substrates became considerably easier.

BIBLIOGRAPHY

[1] S. Ye, Q. Cao, Q. Wang, T. Wang, and Q. Peng, “A highly efficient, stable, durable, and recyclable filter fabricated by femtosecond laser drilling of a titanium foil for oil-water separation,” *Sci Rep*, vol. 6, Nov. 2016, doi: 10.1038/srep37591.

[2] G. Lee, Y. S. Choi, H. J. Yoon, and J. A. Rogers, “Advances in Physicochemically Stimuli-Responsive Materials for On-Demand Transient Electronic Systems,” *Matter*, vol. 3, no. 4. Cell Press, pp. 1031–1052, Oct. 07, 2020. doi: 10.1016/j.matt.2020.08.021.

[3] S. K. Kang, L. Yin, and C. Bettinger, “The emergence of transient electronic devices,” *MRS Bull*, vol. 45, no. 2, pp. 87–95, Feb. 2020, doi: 10.1557/mrs.2020.19.

[4] C. Li *et al.*, “Design of biodegradable, implantable devices towards clinical translation,” *Nature Reviews Materials*, vol. 5, no. 1. Nature Research, pp. 61–81, Jan. 01, 2020. doi: 10.1038/s41578-019-0150-z.

[5] Y. S. Choi *et al.*, “Fully implantable and bioresorbable cardiac pacemakers without leads or batteries,” *Nat Biotechnol*, vol. 39, no. 10, pp. 1228–1238, Oct. 2021, doi: 10.1038/s41587-021-00948-x.

[6] S. Wang *et al.*, “Skin electronics from scalable fabrication of an intrinsically stretchable transistor array,” *Nature*, vol. 555, no. 7694, pp. 83–88, Mar. 2018, doi: 10.1038/nature25494.

[7] S. Il Park *et al.*, “Soft, stretchable, fully implantable miniaturized optoelectronic systems for wireless optogenetics,” *Nat Biotechnol*, vol. 33, no. 12, pp. 1280–1286, Dec. 2015, doi: 10.1038/nbt.3415.

[8] Y.-Q. Zheng *et al.*, “Monolithic optical microlithography of high-density elastic circuits.” [Online]. Available: https://www.science.org

[9] R. Singh, M. J. Bathaei, E. Istif, and L. Beker, “A Review of Bioresorbable Implantable Medical Devices: Materials, Fabrication, and Implementation,”

Advanced Healthcare Materials, vol. 9, no. 18. Wiley-VCH Verlag, Sep. 01, 2020. doi: 10.1002/adhm.202000790.

[10] N. Ashammakhi *et al.*, "Biodegradable Implantable Sensors: Materials Design, Fabrication, and Applications," *Advanced Functional Materials*, vol. 31, no. 49. John Wiley and Sons Inc, Dec. 01, 2021. doi: 10.1002/adfm.202104149.

[11] S. M. Won, L. Cai, P. Gutruf, and J. A. Rogers, "Wireless and battery-free technologies for neuroengineering," *Nature Biomedical Engineering*. Nature Research, Apr. 01, 2021. doi: 10.1038/s41551-021-00683-3.

[12] K. Liu, B. Ouyang, X. Guo, Y. Guo, and Y. Liu, "Advances in flexible organic field-effect transistors and their applications for flexible electronics," *npj Flexible Electronics*, vol. 6, no. 1. Nature Research, Dec. 01, 2022. doi: 10.1038/s41528-022-00133-3.

[13] W. Li *et al.*, "Biodegradable Materials and Green Processing for Green Electronics," *Advanced Materials*, vol. 32, no. 33. Wiley-VCH Verlag, Aug. 01, 2020. doi: 10.1002/adma.202001591.

[14] T. A. Baldo, L. F. De Lima, L. F. Mendes, W. R. De Araujo, T. R. L. C. Paixão, and W. K. T. Coltro, "Wearable and Biodegradable Sensors for Clinical and Environmental Applications," *ACS Applied Electronic Materials*, vol. 3, no. 1. American Chemical Society, pp. 68–100, Jan. 26, 2021. doi: 10.1021/acsaelm.0c00735.

[15] B. Boubellouta and S. Kusch-Brandt, "Relationship between economic growth and mismanaged e-waste: Panel data evidence from 27 EU countries analyzed under the Kuznets curve hypothesis," *Waste Management*, vol. 120, pp. 85–97, Feb. 2021, doi: 10.1016/j.wasman.2020.11.032.

[16] S. M. Yang *et al.*, "Hetero-Integration of Silicon Nanomembranes with 2D Materials for Bioresorbable, Wireless Neurochemical System," *Advanced Materials*, vol. 34, no. 14, Apr. 2022, doi: 10.1002/adma.202108203.

[17] I. A. Paun *et al.*, "Laser micro-patterning of biodegradable polymer blends for tissue engineering," *J Mater Sci*, vol. 50, no. 2, pp. 923–936, Nov. 2014, doi: 10.1007/s10853-014-8652-y.

[18] Y. Yalikun, N. Tanaka, Y. Hosokawa, T. Iino, and Y. Tanaka, "Embryonic body culturing in an all-glass microfluidic device with laser-processed 4 μm thick

ultra-thin glass sheet filter," *Biomed Microdevices*, vol. 19, no. 4, Dec. 2017, doi: 10.1007/s10544-017-0227-7.

[19] M. K. DeBari *et al.*, "Therapeutic Ultrasound Triggered Silk Fibroin Scaffold Degradation," *Adv Healthc Mater*, vol. 10, no. 10, May 2021, doi: 10.1002/adhm.202100048.

[20] K. T. M. Tran *et al.*, "Transdermal microneedles for the programmable burst release of multiple vaccine payloads," *Nat Biomed Eng*, vol. 5, no. 9, pp. 998–1007, Sep. 2021, doi: 10.1038/s41551-020-00650-4.

[21] S. Ye, Q. Cao, Q. Wang, T. Wang, and Q. Peng, "A highly efficient, stable, durable, and recyclable filter fabricated by femtosecond laser drilling of a titanium foil for oil-water separation," *Sci Rep*, vol. 6, Nov. 2016, doi: 10.1038/srep37591.

[22] M. J. Bathaei *et al.*, "Photolithography-Based Microfabrication of Biodegradable Flexible and Stretchable Sensors," *Advanced Materials*, vol. 35, no. 6, Feb. 2023, doi: 10.1002/adma.202207081.

[23] N. Xue *et al.*, "A biodegradable porous silicon and polymeric hybrid probe for electrical neural signal recording," *Sens Actuators B Chem*, vol. 272, pp. 314–323, Nov. 2018, doi: 10.1016/j.snb.2018.06.001.

[24] S. K. Kang *et al.*, "Bioresorbable silicon electronic sensors for the brain," *Nature*, vol. 530, no. 7588, pp. 71–76, Feb. 2016, doi: 10.1038/nature16492.

[25] S. H. C. Anderson, H. Elliott, D. J. Wallis, L. T. Canham, and J. J. Powell, "Dissolution of different forms of partially porous silicon wafers under simulated physiological conditions," in *Physica Status Solidi (A) Applied Research*, May 2003, pp. 331–335. doi: 10.1002/pssa.200306519.

[26] D. Choi *et al.*, "Recent Advances in Triboelectric Nanogenerators: From Technological Progress to Commercial Applications," *ACS Nano*. American Chemical Society, 2022. doi: 10.1021/acsnano.2c12458.

[27] T. Thambi, V. H. Giang Phan, S. H. Kim, T. M. Duy Le, H. T. T. Duong, and D. S. Lee, "Smart injectable biogels based on hyaluronic acid bioconjugates finely substituted with poly(β-amino ester urethane) for cancer therapy," *Biomater Sci*, vol. 7, no. 12, pp. 5424–5437, Dec. 2019, doi: 10.1039/c9bm01161g.

[28] M. I. H. Mondal and F. Ahmed, "Cellulosic fibres modified by chitosan and synthesized ecofriendly carboxymethyl chitosan from prawn shell waste,"

Journal of the Textile Institute, vol. 111, no. 1, pp. 49–59, Jan. 2020, doi: 10.1080/00405000.2019.1669321.

[29] K. Kenry and B. Liu, "Recent Advances in Biodegradable Conducting Polymers and Their Biomedical Applications," *Biomacromolecules*, vol. 19, no. 6. American Chemical Society, pp. 1783–1803, Jun. 11, 2018. doi: 10.1021/acs.biomac.8b00275.

[30] S. K. Kang, J. Koo, Y. K. Lee, and J. A. Rogers, "Advanced Materials and Devices for Bioresorbable Electronics," *Acc Chem Res*, vol. 51, no. 5, pp. 988–998, May 2018, doi: 10.1021/acs.accounts.7b00548.

[31] T. Lei *et al.*, "Biocompatible and totally disintegrable semiconducting polymer for ultrathin and ultralightweight transient electronics," *Proc Natl Acad Sci U S A*, vol. 114, no. 20, pp. 5107–5112, May 2017, doi: 10.1073/pnas.1701478114.

[32] R. J. Zomer *et al.*, "Global Tree Cover and Biomass Carbon on Agricultural Land: The contribution of agroforestry to global and national carbon budgets," *Sci Rep*, vol. 6, Jul. 2016, doi: 10.1038/srep29987.

[33] Q. Zhang, Y. Yan, S. Li, and T. Feng, "The synthesis and characterization of a novel biodegradable and electroactive polyphosphazene for nerve regeneration," *Materials Science and Engineering C*, vol. 30, no. 1, pp. 160–166, Jan. 2010, doi: 10.1016/j.msec.2009.09.013.

[34] J. F. Zhou, Y. G. Wang, L. Cheng, Z. Wu, X. D. Sun, and J. Peng, "Preparation of polypyrrole-embedded electrospun poly(lactic acid) nanofibrous scaffolds for nerve tissue engineering," *Neural Regen Res*, vol. 11, no. 10, pp. 1644–1652, Oct. 2016, doi: 10.4103/1673-5374.193245.

[35] E. S. Hosseini, S. Dervin, P. Ganguly, and R. Dahiya, "Biodegradable Materials for Sustainable Health Monitoring Devices," *ACS Applied Bio Materials*, vol. 4, no. 1. American Chemical Society, pp. 163–194, Jan. 18, 2021. doi: 10.1021/acsabm.0c01139.

[36] S. W. Hwang *et al.*, "Materials for bioresorbable radio frequency electronics," *Advanced Materials*, vol. 25, no. 26, pp. 3526–3531, Jul. 2013, doi: 10.1002/adma.201300920.

[37] S. Paik *et al.*, "Near-field sub-diffraction photolithography with an elastomeric photomask," *Nat Commun*, vol. 11, no. 1, Dec. 2020, doi: 10.1038/s41467-020-14439-1.

[38] A. Kumar and G. M. Whitesides, “Features of gold having micrometer to centimeter dimensions can be formed through a combination of stamping with an elastomeric stamp and an alkanethiol ‘ink’ followed by chemical etching,” *Appl Phys Lett*, vol. 63, no. 14, pp. 2002–2004, 1993, doi: 10.1063/1.110628.

[39] “The spectacularly successful fabrication techniques,” 2005.

[40] G. Raciukaitis, “Ultra-Short Pulse Lasers for Microfabrication: A Review,” *IEEE Journal of Selected Topics in Quantum Electronics*, vol. 27, no. 6, Nov. 2021, doi: 10.1109/JSTQE.2021.3097009.

[41] H. Mirzajani *et al.*, “An ultra-compact and wireless tag for battery-free sweat glucose monitoring,” *Biosens Bioelectron*, vol. 213, Oct. 2022, doi: 10.1016/j.bios.2022.114450.

[42] S. Ravi-Kumar, B. Lies, X. Zhang, H. Lyu, and H. Qin, “Laser ablation of polymers: a review,” *Polymer International*, vol. 68, no. 8. John Wiley and Sons Ltd, pp. 1391–1401, Aug. 01, 2019. doi: 10.1002/pi.5834.

[43] A. Carlson, A. M. Bowen, Y. Huang, R. G. Nuzzo, and J. A. Rogers, “Transfer printing techniques for materials assembly and micro/nanodevice fabrication,” *Advanced Materials*, vol. 24, no. 39. pp. 5284–5318, Oct. 09, 2012. doi: 10.1002/adma.201201386.

[44] C. Linghu, S. Zhang, C. Wang, and J. Song, “Transfer printing techniques for flexible and stretchable inorganic electronics,” *npj Flexible Electronics*, vol. 2, no. 1. Nature Research, Dec. 01, 2018. doi: 10.1038/s41528-018-0037-x.

[45] H. J. Kim-Lee, A. Carlson, D. S. Grierson, J. A. Rogers, and K. T. Turner, “Interface mechanics of adhesiveless microtransfer printing processes,” *J Appl Phys*, vol. 115, no. 14, Apr. 2014, doi: 10.1063/1.4870873.

[46] M. C. Dang, T. M. Dung Dang, and E. Fribourg-Blanc, “Inkjet printing technology and conductive inks synthesis for microfabrication techniques,” *Advances in Natural Sciences: Nanoscience and Nanotechnology*, vol. 4, no. 1, 2013, doi: 10.1088/2043-6262/4/1/015009.

[47] B. J. De Gans, P. C. Duineveld, and U. S. Schubert, “Inkjet printing of polymers: State of the art and future developments,” *Advanced Materials*, vol. 16, no. 3. Wiley-VCH Verlag, pp. 203–213, Feb. 03, 2004. doi: 10.1002/adma.200300385.

[48] D. Attinger, Z. Zhao, and D. Poulikakos, “An Experimental Study of Molten Microdroplet Surface Deposition and Solidification: Transient Behavior and

Wetting Angle Dynamics," 2000. [Online]. Available: http://heattransfer.asmedigitalcollection.asme.org/

[49] K. Y. Mitra, A. Willert, R. Chandru, R. R. Baumann, and R. Zichner, "Inkjet Printing of Bioresorbable Materials for Manufacturing Transient Microelectronic Devices," *Adv Eng Mater*, vol. 22, no. 12, Dec. 2020, doi: 10.1002/adem.202000547.

[50] O. Vazquez-Mena, L. Gross, S. Xie, L. G. Villanueva, and J. Brugger, "Resistless nanofabrication by stencil lithography: A review," *Microelectronic Engineering*, vol. 132. Elsevier B.V., pp. 236–254, Jan. 25, 2015. doi: 10.1016/j.mee.2014.08.003.

[51] K. Du, J. Ding, Y. Liu, I. Wathuthanthri, and C. H. Choi, "Stencil lithography for scalable micro- and nanomanufacturing," *Micromachines*, vol. 8, no. 4. MDPI AG, Apr. 19, 2017. doi: 10.3390/mi8040131.

[52] M. Liu *et al.*, "Terahertz-field-induced insulator-to-metal transition in vanadium dioxide metamaterial," *Nature*, vol. 487, no. 7407, pp. 345–348, Jul. 2012, doi: 10.1038/nature11231.

[53] T. Deng, M. Li, J. Chen, Y. Wang, and Z. Liu, "Controllable fabrication of pyramidal silicon nanopore arrays and nanoslits for nanostencil lithography," *Journal of Physical Chemistry C*, vol. 118, no. 31, pp. 18110–18115, Aug. 2014, doi: 10.1021/jp503203b.

[54] P. B. Agarwal, S. Pawar, S. M. Reddy, P. Mishra, and A. Agarwal, "Reusable silicon shadow mask with sub-5 μm gap for low cost patterning," *Sens Actuators A Phys*, vol. 242, pp. 67–72, May 2016, doi: 10.1016/j.sna.2016.02.040.

[55] M. Huff, "Recent advances in reactive ion etching and applications of high-aspect-ratio microfabrication," *Micromachines (Basel)*, vol. 12, no. 8, Aug. 2021, doi: 10.3390/mi12080991.

[56] M. D. Henry, C. Welch, and A. Scherer, "Techniques of cryogenic reactive ion etching in silicon for fabrication of sensors," *Journal of Vacuum Science & Technology A: Vacuum, Surfaces, and Films*, vol. 27, no. 5, pp. 1211–1216, Sep. 2009, doi: 10.1116/1.3196790.

[57] J. Yeom, Y. Wu, J. C. Selby, and M. A. Shannon, "Maximum achievable aspect ratio in deep reactive ion etching of silicon due to aspect ratio dependent transport and the microloading effect," *Journal of Vacuum Science & Technology*

B: Microelectronics and Nanometer Structures, vol. 23, no. 6, p. 2319, Nov. 2005, doi: 10.1116/1.2101678.

[58] "https://www.brewerscience.com/products/advanced-lithography/photolithography-process/."

[59] "https://www.ulsinc.com/learn/laser-material-processing#:~:text=or%20material%20modification.-,Material%20Ablation,laser%20engraving%2C%20and%20laser%20drilling."

[60] M. Pedersen and M. Huff, "Plasma Etching of Deep High-Aspect Ratio Features into Fused Silica," *Journal of Microelectromechanical Systems*, vol. 26, no. 2, pp. 448–455, Apr. 2017, doi: 10.1109/JMEMS.2017.2661959.